Quantum-chemistry based calibration of the alkali metal cation series (Li+– Cs+) for large-scale polarizable molecular mechanics/dynamics simulations.

Journal:	*Journal of Computational Chemistry*
Manuscript ID:	JCC-14-0479.R1
Wiley - Manuscript type:	Full Paper
Date Submitted by the Author:	05-Nov-2014
Complete List of Authors:	Gresh, Nohad; CNRS, Meuwly, Markus; University of Basel, Devereux, Michael; University of Basel, Piquemal, Jean-Philip; Laboratoire de Chimie Theorique, Chemistry; Lim, Carmay; Academia Sinica, Institute of Biomedical Sciences; Dudev, Todor; University of Sofia,
Key Words:	Alkali metal cations, O, N, S, and Se ligands, Energy decomposition, Quantum chemistry, Polarizable molecular mechanics

SCHOLARONE™
Manuscripts

In the context of the SIBFA polarizable molecular mechanics procedure, the alkali cations in the series Li+-Cs+ are calibrated and validated. This is done upon referring to *ab initio* quantum-chemical (QC) calculations at the aug-cc-pVTZ(-f) level, with representative O, N, S, and Se-ligands. The validations are done on several polycoordinated complexes of these cations, and a close reproduction of the QC results can be obtained.

Figure 7b

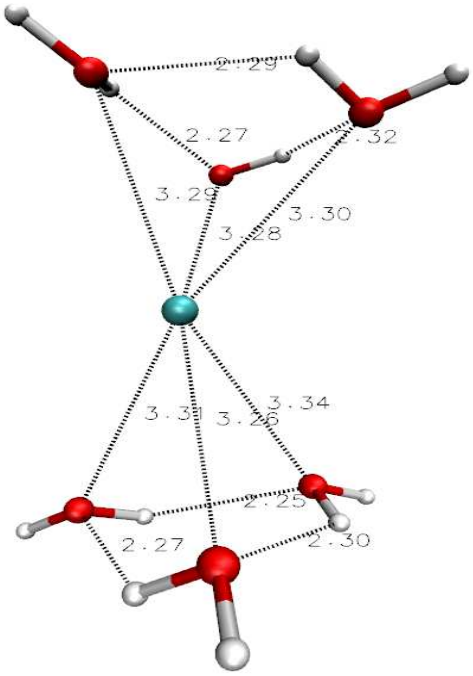

Quantum-chemistry based calibration of the alkali metal cation series (Li^+–Cs^+) for large-scale polarizable molecular mechanics/dynamics simulations.

Todor Dudev, [a] Mike Devereux,[b] Markus Meuwly,[b] Carmay Lim,[c] Jean-Philip Piquemal,[d] Nohad Gresh[e]

[a]Faculty of Chemistry and Pharmacy, University of Sofia, 1164 Sofia, Bulgaria

[b]Department of Chemistry, University of Basel

[c]Institute of Biomedical Sciences, Academia Sinica, Taipei 115, Taiwan and Department of Chemistry, National Tsing Hua University, Hsinchu 300 Taiwan

[d]Laboratoire de Chimie Théorique, Sorbonne Universités, UPMC, UMR7616 CNRS, Paris, France

[e] Chemistry & Biology, Nucleo(s)tides & Immunology for Therapy (CBNIT), CNRS UMR8601, Université Paris Descartes, PRES Sorbonne Paris Cité, UFR Biomédicale, 45 rue des Saints-Pères, 75270 Paris Cedex 06, France

Summary. The alkali metal cations in the series Li^+ – Cs^+ act as major partners in a diversity of biological processes and in bioinorganic chemistry. In this paper we present the results of their calibration in the context of the SIBFA polarizable molecular mechanics/dynamics procedure. It relies on quantum-chemistry (QC) energy-decomposition analyses of their mono-ligated complexes with representative O-, N-, S- and Se- ligands, performed with the aug-cc-pVTZ(-f) basis set at the Hartree-Fock (HF) level. Close agreement with QC is obtained for each individual contribution, even though the calibration involves only a limited set of cation-specific parameters. This agreement is preserved in tests on polyligated complexes with four and six O-ligands, water and formamide, indicating the transferability of the procedure. Preliminary extensions to density functional theory calculations are reported.

Keywords. Alkali metal cations. O, N, S, and Se ligands. Energy decomposition, quantum chemistry, polarizable molecular mechanics.

For Peer Review

Introduction

The present work bears on the calibration of the Li^+ - Cs^+ alkali metal cations in the context of the SIBFA molecular mechanics procedure, which relies on distributed multipoles and polarizabilities. It is strongly motivated by the involvement of these cations in numerous processes, which cover biology, organic and bioinorganic chemistry, and material science. Li^+, a non-biogenic element, is used in the treatment of psychiatric diseases, such as bipolar disorder , and chronic neurodegenerative diseases such as Alzheimer's, Parkinson's, and Huntington's diseases [1]. One of its therapeutic effects is to replace Mg^{2+} in enzymes involved in bipolar disorder such as glycogen synthase kinase 3 beta [2, 3]. The whole set of proteins prone to lithium attack, which are potential drug targets, has yet to be identified. Na^+ and K^+ relay the action of neurotransmitters by passage through transmembrane ion channels following membrane depolarization [for recent reviews, see 4, 5, 6]. These ion channels are involved in regulating the homeostasis of blood and body fluids, cardiac, skeletal, and smooth muscle contraction, taste and pain sensation, and signal transduction [7]. Na^+ and K^+ are also essential for the stabilization of guanine tetramers, which are found in non-standard DNA structures such as telomeres [8, 9], and are used to construct G4 nanowires [10]. Rb^+ isotopes are used in radiopharmaceutical reagents [11] and Cs^+ is found in nuclear waste or in fission products [12]. Due to their chemical similarity to potassium, they can compete with it, and penetrate and accumulate in living tissues [reviewed in 13].

It is very important but also challenging to understand the energy basis for selective recognition of one cation of the series over the others. This is exemplified by ion channel proteins, and is motivated by the fact that a few of them have been resolved by X-ray crystallography [for recent examples, see, e.g., 4, 14, 15, 16]. But it could also be extremely rewarding to design macrocylic hosts that can selectively entrap and transport a targeted cation [see, eg. 17, 18, 19]. Along with the enthalpy of binding of the cation to its target, the calculation of the stabilization energies needs to include the desolvation energy of the cation and of the target prior to complexation, and to embody entropy. Along these lines, calculation of such energies in the context of ab initio quantum-chemistry (QC) combined with continuum dielectric calculations have helped to unravel the factors governing the relative K^+ and Na^+ affinities in models of the selectivity filters of K^+ [20] and Na^+ [21a,b] channels. However, because QC calculations are computer-intensive, they are limited to relatively small model systems. To perform long molecular dynamics (MD)

John Wiley & Sons, Inc.

simulations on very large systems such as ion channels, telomeric DNA, or large-sized macrocycles, it is necessary to resort to 'empirical' potentials. Due to the strong polarizing fields exerted by the cation, it is preferable to explicitly include second-order contributions, namely polarization and charge-transfer. More specifically, polarizable force-fields with a Drude model have been developed to include this contribution [22] and subsequently used to simulate ion channels [23]

A reliable force field should closely reproduce available experimental data, as well as the results of QC computations in diverse model systems so as to extend their realm to very large complexes not amenable to QC, and/or to long MD simulations. Such a goal could be attained if each of the separate contributions of the QC intermolecular interaction energy had its counterpart in molecular mechanics. Such QC contributions could be unraveled for operational purposes by energy-decomposition schemes. The calibration on monoligated complexes is not done to reproduce experimental values, but these individual contributions. It is essential to evaluate whether, with a minimal calibration effort, the MM potential can retain a balance as close as possible to QC of these individual contributions upon varying the ligands and the cations, and upon passing from mono- to polyligated complexes. This is a prerequisite for the transferability of the potential [24], but also for subsequent comparison with available experimental results, such as those available for the polyhydrated complexes of these cations on the one hand and their bulk solvation energies on the other hand [25]. Such comparisons are planned after inclusion of both correlation and dispersion effects is achieved in a subsequent step to the present study. We focus here on mono- and polyligated complexes at the Hartree-Fock level, and the extension to correlated calculations is limited to mono-ligated complexes. It has to be noted that since extensions to polyligated complexes at the correlated level will be benchmarked by dispersion-augmented DFT calculations, the accuracy of the potential could be limited by that of the QC calculations.

Along these lines, the SIBFA procedure [24], which has such a separable energy formulation, has been extended to several metal cations, namely: the alkaline-earth cations, Mg(II) and Ca(II) [26], the transition metals Zn(II) [27 a-b], Cu(I) [28], and Cu(II) [29]; toxic metals Pb(II) [30] and Hg(II) [31], and lanthanides and actinides [32]. Earlier versions of this method and of its forerunners have already dealt with the series Na^+ – Cs^+. Na^+ and K^+ have been calibrated in our previous studies, which resorted to distributed QC multipoles along with scalar polarizabilities

[33 a, b]. This method can successfully account for the K^+ versus Na^+ selectivity of the valinomycin [34] and nonactin [35] ionophores, and, conversely, of the Na^+ versus K^+ preferences by nigericin [36]. It has been used in the first polarizable molecular mechanics modeling of the passage of cations through the gramicidin transmembrane channel [37a, b]. It can account for the observed preference of $Rb^+ > K^+ > Cs^+ > Na^+$ for the binding between two stacked guanine tetramers [38].

We are constructing a new library of SIBFA constitutive fragments with distributed multipoles and polarizabilities derived with the aug-cc-pVTZ(-f) basis set [39]. This study presents the results of the calibration of the Li^+ – Cs^+ cations with this basis set and its validation in several test cases in view of large-scale simulations. Along with the use of this extended Gaussian basis set rather than the smaller basis sets used in these earlier studies, this update is necessary because of the refinements of each energy contribution to the SIBFA potential [reviewed in Ref. 24]. It deals principally with O-containing ligands, to which alkali cations bind predominantly [40]. We will specifically consider water, methanol, formamide, and formate. The last three ligands model the Ser/Thr, Asn/Gln, and Asp/Glu side-chains, respectively. Formamide is also the main building block of the protein main-chain. In order to have a 'universal' calibration, we will also consider N-, S-, and Se-containing ligands. N-ligands are modeled by imidazole, which models the His side-chain, pyridine, and trimethylamine; these three ligands are frequently encountered as building blocks of supramolecular guests. S-ligands are modeled by methylthiolate and thioether, which model the Cys^- and Met side-chains, respectively. Se-containing ligands are similarly modeled by methylselenothiolate and selenomethionine, modeling the selenocysteinate and selenomethionine side-chains, which are the selenium derivatives of Cys^- and Met residues, respectively, encountered in some enzymes such as glutathione transferase. The present calibrations will deal solely with cation-specific parameters, as the ligand-specific parameters (vide infra) have been calibrated in a previous study for water, formamide, and imidazole [39] by a fitting scheme to QC results with the interactive non-linear least squares fitting (I-NoLLS) software [39, 41, 42]; the other ligands were calibrated beforehand by manual fitting in order to reproduce the results from energy-decomposition analyses for their complexation by a Mg(II) probe (unpublished results). This was done on monoligated complexes only upon performing distance variations.

John Wiley & Sons, Inc.

Throughout this study we will denote by M^+ any of the Li^+ – Cs^+ cations. We will perform energy decomposition analyses upon distance variations of an alkali cation approaching water, imidazole, methylthiolate and methylselenothiolate. The distance dependencies in each M^+–water complex will first enable calibration of the effective cation radii used to compute the individual SIBFA contributions. This is done so that the radial decay of each contribution parallels that of its QC counterpart. The dependencies in these four complexes will then enable calibration of the M^+–O, M^+–N, M^+–S, and M^+–Se atom-number dependent pairwise coefficients used to compute the repulsion contribution, so that the SIBFA repulsion contribution, E_{rep}, matches the QC exchange-repulsion contribution, EX, at and near equilibrium distance. The H–M^+ and C–M^+ coefficients will be calibrated on the M^+–water and M^+–formamide complexes. They are less critical since H and C atoms are more remote from the cation. The distance variations in the other complexes will serve as tests for the transferability of the method. More demanding tests will involve representative polyligated M^+ complexes with four or six ligands. Specifically, we will consider a) M^+ complexes with four and with six water molecules in two competing arrangements, namely coplanar and the pyramidal for tetrahydrated complexes, and octahedral and the bipyramidal for hexahydrated complexes; b) M^+ complexes with four and with six formamides. Single-point computations will be done on the SIBFA energy-minimized structures and the results compared to energy decomposition analyses. This will help to quantify the weight of each QC energy contribution within the total intermolecular interaction energy, ⍰E, its impact on the stabilization of the competing structures, and how well all these features could be reproduced by SIBFA. In the last section of this study, using the B3-LYP DFT functional, we will evaluate the impact of correlation on the interaction energies and their contributions to representative complexes, and how these could be accounted for by the use of correlated multipoles and polarizabilities.

Methods

1) QC computations

The energy decompositions were done with the Reduced Variational Space analysis (RVS) of Stevens and Fink [43]. This procedure separates the total interaction energy into four contributions: the first order (E_1) Coulomb (EC) and short-range exchange-repulsion (EX) and second order (E_2) polarization (POL) and charge-transfer (CT). The Basis Set Superposition Error [44 a,b] was evaluated within the virtual orbital space. We used the GAMESS software [45] and the aug-cc-pVTZ(-f) basis set [46a, b]. The intermolecular interaction energies ΔE were computed at the correlated level with the B3LYP [47] functional using the Constrained Space Orbital Variation Analysis (CSOV) [48] coded with the Hondo/98 software [49]. Stuttgart effective core potentials [50] were used on the heavier atoms K^+, Rb^+, and Cs^+.

2) SIBFA computations

In the SIBFA procedure [24], the intermolecular interaction energy is computed as the sum of five contributions: electrostatic multipolar (E_{MTP*}), short-range repulsion (E_{rep}), polarization (E_{pol}), charge transfer (E_{ct}), and dispersion (E_{disp})

$$\Delta E_{TOT} = E_{MTP} + E_{rep} + E_{pol} + E_{ct} + E_{disp} \quad (1)$$

E_{MTP} was computed with distributed multipoles (up to quadrupoles) derived from the QC molecular orbitals precomputed for each individual molecule and augmented with an overlap-dependent penetration term [51]. The multipoles were derived from the Stone GDMA analysis [52a, b] and distributed on the atoms and the bond barycenters using a procedure developed by Vigné-Maeder and Claverie [53]. This was done by a home-built routine [Devereux, M., Paris, 2010]. In the case of formamide, we resorted to a newly-developed procedure [54; and Devereux et al., 2014], in which the multipoles were derived from a least-squares fit to the electrostatic potential generated by its electronic density, as these improved reproduction of EC compared to those derived by the GDMA analysis. A net monopolar charge of one is used on the cations. The anisotropic polarizabilities were distributed on the centroids of the localized orbitals (heteroatom lone pairs and bond barycenters) using a procedure due to Garmer and Stevens [55]. E_{rep} and E_{ct}, the two short-range contributions, were computed using representations of the molecular orbitals localized on the chemical bonds and on localized lone pairs. The distributed polarizabilities at

For Peer Review

the correlated level were computed with an in-house version of Hondo/98 [Piquemal, J.-P., Giessner-Prettre, C., unpublished]. Energy-minimizations used the polyvalent 'Merlin' minimizer [56].

Results and Discussion

I. Monoligated complexes. Tables I–V list the results for Li^+, Na^+, K^+, Rb^+, and Cs^+, whereas Figures 1–5 compare the radial evolution of ΔE(QC) and ΔE(SIBFA) and their contributions for the Li^+–water, Na^+–formate, K^+–formamide, Rb^+–imidazole, and Cs^+–methanethiolate complexes, respectively. The approaches of the cations to water, imidazole, pyridine, methylamine, methanethiol and selenothiol are along the external bisectors of the bound heteroatom. In the formamide complexes, the M-O-C angle is 165°. In the methanethiolate and selenothiolate complexes, the M-S/Se-C angle is 104.5°. Two complexes with formate were considered: the bidentate complex, in which the cation bridges both O atoms at equal distances, and an 'external' complex, in which it binds in a monodentate fashion to one O atom, the M-O-C angle being 120°, the corresponding M-O being *cis* to the HC bond.

The K(M+–N) E_{rep} multiplicative constants are given in the Appendix. An unexpectedly small value for the Cs-Se pairwise interaction was obtained, for which at present there is no clear explanation.

Li^+ complexes (Table I and Figure 1). The calibration on the Li^+–water complex enabled a close fit of all four HF contributions at equilibrium distance (1.8 Å). The value of ΔE(HF) of –34.5 kcal/mol is virtually identical to the 6-31+G* Restricted Hartree-Fock (RHF) one published by Glendening and Feller [57], and close to the experimental ΔH value of –34.0 kcal/mol [25, 58], but slightly larger than the aug-cc-pVDZ value of –32.8 kcal/mol of Miller and Lisy [57]. The radial evolutions of these contributions, shown in Figure 1, are well accounted for. The agreement between SIBFA and QC values carries over well to the methanol and formate complexes. With formate, there is a slight tendency to underestimate the relative stabilization of the bidentate versus the monodentate complexes, which amounts to 22 kcal/mol in SIBFA compared to 26 kcal/mol in QC. The least favorable agreement for the O-ligands is for the formamide complex, where ΔE(SIBFA) underestimates ΔE(HF) by 6.3 kcal/mol out of 54 kcal/mol due to an underestimation of EC by E_{MTP}* and an overestimation of E_{exch} by E_{rep}. This

For Peer Review

complex along with that of Li^+ with selenocysteinate (vide infra) turns out to be the least satisfactory in the whole series of mono-ligated alkali metal complexes.

Satisfactory agreement was obtained with the N- and S- ligands. For the N-ligands, E_{MTP} tends to slightly underestimate EC, a tendency that increases upon passing from imidazole to pyridine and trimethylamine. Note that the calibration was based on the Li^+–imidazole complex involving the sole K(Li–N) E_{rep} multiplicative constant. E_{pol}(SIBFA) slightly overestimates E_{pol}(QC), thus compensating for the inverse trend of E_{MTP}, while E_{rep} matches closely E_{exch} with all three ligands. The calibration of the K(Li–S) E_{rep} multiplicative constant done on Li^+–methanethiolate enabled a close reproduction of ΔE(QC) in the Li^+–methionine complex. In the Li^+–selenocysteinate complex, E_{pol}(SIBFA) overestimated E_{pol}(QC), as a result of which ΔE(SIBFA) overestimated ΔE(QC) by a rather large amount, 17.5 kcal/mol out of 146 kcal/mol. This might be because the SIBFA E_{pol} parameters for selenocysteinate were previously determined by studying its complex with a Mg(II) probe, which had a comparable equilibrium distance to that of Li^+ (2.20 as compared to 2.30 Å). In the Li^+–selenomethionine complex, E_{pol}(SIBFA) also overestimated E_{pol}(QC) but by a lesser amount, and a more satisfactory overall agreement was obtained in terms of the total energies (1.6 out of 28 kcal/mol).

Na^+ complexes (Table II and Figure 2). For the O-ligands, much closer agreement between SIBFA and QC computations was obtained than with Li^+, in terms of both the total energies and their individual contributions. For Na^+–water, the value of ΔE(QC) (–23.8 kcal/mol) is close to the QC value of Glendening and Feller [56] (–24.4 kcal/mol), larger than the QC value of Miller and Lisy [59] (–22.2 kcal/mol), and close to the experimental ΔH value (–24.0 kcal/mol) [58]. Compared to the Li^+–formate complex, the tendency to underestimate the stability of the bidendate complex with respect to the monodentate one has been attenuated (20.7 kcal/mol as compared to 23.4 kcal/mol in QC). ΔE(SIBFA) can match ΔE(QC) with relative errors < 2%.

Close agreement was also obtained with the N-, S- and Se-ligands. The least satisfactory ligand is trimethylamine, with an error of 4.4 kcal/mol out of 27 kcal/mol. As found for the Li^+–selenocysteinate complex, E_{pol}(SIBFA) is also overestimated with respect to E_{pol}(QC) in the Na^+–selenocysteinate complex, but the overestimation is reduced (6.9 kcal/mol instead of 14.1 kcal/mol), and compensates for the corresponding underestimation of E_1. In this and in the following examples, deviations of ΔE(SIBFA) with respect to ΔE(HF) can be seen starting at <

For Peer Review

0.10 Å from equilibrium distance. Their impact could be limited, however, because in polyligated complexes, the M^+ – ligand equilibrium distances are in the general case shifted to larger values due to ligand-ligand repulsions, shielding of the cation-generated field on any one ligand by the fields generated by the other ligands, and limited mobility of the ligands due to their anchoring in larger molecular entities.

K^+ complexes (Table III and Figure 3). For water–K^+, the ΔE(QC) of –16 kcal/mol is close to that obtained by Miller and Lisy (–15.2 kcal/mol) [59], but is less negative than that computed by Glendening and Feller (–18 kcal/mol) [57], which is nearly identical to the experimental value of –17.9 kcal/mol [58]. For O-ligands, the agreement is even better than the agreement obtained for Na^+ complexes. In the case of formate, the SIBFA preference for bi- versus monodentate binding was even closer to the corresponding QC difference (20 kcal/mol versus 21.5 kcal/mol).

Close agreement is also found with the N-, S-, and Se-ligands. The trimethylamine complex could still be considered as less satisfactory. The apparently ideal agreement of ΔE(SIBFA) with ΔE(QC) results from some error compensation, the underestimation of E_1(QC) being compensated by an overestimation of E_{pol}(QC) by E_{pol}(SIBFA). The same situation holds for the K^+ complex with the Se-ligands.

Rb^+ complexes (Table IV and Figure 4). With the O-ligands, the agreement between SIBFA and QC results has a quality comparable to that found with K^+: Good agreement is also found with the N- and S-ligands, with trimethylamine again yielding the least favorable agreement, with the previously observed underestimation of E_1 and overestimation of E_{pol} by their SIBFA counterparts. Whereas a close agreement is seen with neutral selenomethionine, significant error compensation occurs with selenocysteinate. The first-order EC and E_{exch} contributions are under- and overestimated, respectively, by their SIBFA counterparts, while both second-order contributions are overestimated. The compensation of errors left a residual error of 4.5 kcal/mol out of 97 kcal/mol.

Cs^+ complexes (Table V and Figure 5). For water–Cs^+, the value of the interaction energy (–12.2 kcal/mol) is larger than the one computed by Miller and Lisy [59], but smaller than the experimental value (–13.7 kcal/mol) [58]. With the O-ligands, the close agreement between SIBFA and QC found along the Na^+–Rb^+ series is retained, although ΔE(QC) for both formate complexes is underestimated by ΔE(SIBFA) by 4–7 kcal/mol out of 100, which is slightly larger

John Wiley & Sons, Inc.

For Peer Review

than the corresponding difference in Rb^+ complexes (3–4 kcal/mol). The trends found for the Rb^+ complexes containing N-, S-, and Se- ligands also apply to the corresponding Cs^+ complexes.

Metal selectivity

Based on the present QC and SIBFA results, it is of particular interest to assess the affinities and discriminative powers of the ligands studied toward the group IA monocations. As expected, charged ligands (formate, methanethiolate, and methaneselenate), due to strong charge–charge interactions, secure the highest binding energies in the series ranging from ~ –170 to ~ –90 kcal/mol. The complexes between metal cations and neutral ligands are characterized by smaller binding energies on the order of tens of kcal/mol. As compared to their uncharged counterparts, the gas-phase charged ligands appear to be more selective toward the monocations studied: in going down group IA, the binding energies of anionic ligands vary over a wider range (up to ~60 kcal/mol between Li^+ and Cs^+ complexes) than those of the neutral ligands (~30 kcal/mol, respectively). A similar trend has been observed for the series of divalent transition metals (Co^{2+}, Ni^{2+}, Cu^{2+}, Zn^{2+}, Cd^{2+} and Hg^{2+}), where models of negatively charged Asp^-/Glu^- and Cys^- ligands exhibited the highest metal selectivity [60]. Interestingly, the "soft" Cys^- ligand appeared to be more selective than the "harder" Asp^-/Glu^- in the series of transition divalent metals, but it appears to be as selective as Asp^-/Glu^- ligands in the series of "harder" monovalent cations. The relative deviations in binding energies found for the methanethiolate and formate complexes (Tables I–V) are similar to those found with the Cys^- and Asp^-/Glu^- ligands .

II. Polyligated complexes

a) Water ligands. The results are reported in Tables VI(a-e) for the five cations. Although previous publications [57] have already considered such complexes, none to our knowledge has unraveled the energy contributions responsible for the preferences between the competing structures. As in our previous papers [61, 27b, 62] we report two values for E_{pol}. For the QC calculations, these are E_{pol}(RVS), in which each monomer is relaxed in succession while the other monomers are frozen and variational E_{pol}(VR), in which all monomers are relaxed simultaneously. It is computed as the difference between ΔE(HF) and the sum of E_1 and E_{ct}. For the SIBFA calculations, the two corresponding values are E_{pol*} in which each monomer is subjected to the field exerted by the permanent multipoles of all the other monomers; and E_{pol}, at the outcome of an iterative procedure, in which it is subjected to a field augmented by the ones

For Peer Review

exerted by the induced dipoles on the others. E_{pol*} and E_{pol} are to be compared to E_{pol}(RVS) and E_{pol}(VR), respectively.

Tetraligated complexes. Figures 6a and 6b depict the structures of the representative $Li^+(H_2O)_4$ complex in planar and pyramidal geometry, respectively. The ΔE(QC) values in Tables VIa–VIe show that for small cations (Li^+ and Na^+), the pyramidal complex is more stable than the planar one owing to both E_1 and E_2 contributions but for larger cations (K^+, Rb^+, and Cs^+), the ΔE(QC) values are ≤ ~1 kcal/mol, indicating no significant preference for either geometry. ΔE(SIBFA) reproduces ΔE(QC): for all five complexes, the relative errors in its magnitude with respect to the corresponding ΔE(QC) values are <2%, and the trends of the individual contributions are faithfully reproduced.

Hexaligated complexes. Figures 7a and 7b illustrate the structures of the octahedral and trigonal bipyramidal complexes of $Cs^+(H_2O)_6$. A distinctive feature of the bipyramidal complexes, denoted as 6(S6) in [57], is the formation of two separate cyclic water trimers each stabilized by three H-bonds, while the six O atoms bind the central cation. There is an interplay between attractive water–cation and water–water interactions, and repulsive O–O interactions. The results in Tables VIa-e show that all the octahedral complexes are invariably favored by E_1, and the bipyramidal ones by E_2. Within E_1, the preference of EC for bipyramidal complexes is always overcome by a more unfavorable E_{rep}. For Li^+, the octahedral complex has significantly less positive short-range repulsion energy than the bipyramidal complex, hence it is preferred over the bipyramidal one by 5.5 (QC) and 8.8 (SIBFA) kcal/mol. However, Na^+ and K^+ exhibit no significant difference (≤1.6 kcal/mol) between octahedral and trigonal bipyramidal geometries. For even larger cations, the bipyramidal complex becomes favored by ~2 kcal/mol for Rb^+ and by ~3 kcal/mol for Cs^+ out of ~65 and ~60 respectively. For all complexes, the numerical values of ΔE(SIBFA) match those of ΔE(QC) with a relative error < 3%.

E_{ct}(QC), and not only E_{pol}(QC), plays a role within E_2 in the preferential stabilization of the bipyramidal structure. Its magnitude is the largest in the Li^+ complex due to two effects: (i) charge transfer from each of the water ligands to Li^+, which is the sole alkali cation giving rise to a significant E_{ct} value in the monohydrated complexes, and (ii) charge transfer due to the three H-bonding interactions in each of the two cyclic dimers. E_{ct} in the bipyramidal structures is smaller for the other four cations, but it remains systematically larger than that in the octahedral

For Peer Review

complexes where there are no H-bonding interactions among the cation-ligating water molecules. E_{ct} is thus seen to contribute, along with E_{pol}, to the preference of the larger cations, Rb^+, and Cs^+, in favor of the bipyramidal arrangement.

The many-body effects due to non-additivity, upon passing from mono- to polyligated complexes, stem essentially from E_{pol} and E_{ct}. They were unraveled in a preceding paper which bore on polyligated complexes of Zn(II), where it was shown that the results from QC computations were correctly accounted for using SIBFA [61]. The magnitudes of E_{pol}(QC) and E_{ct}(QC) are also correctly retrieved here in SIBFA upon passing from the mono- to the tetra- and hexahydrated complexes of the alkali cations. This implies a proper control of non-additivity in such complexes as well.

b) Formamide ligands

Tetramers. The five complexes are represented in Figures 8(a-e) and the results are reported in Table VII. Energy-minimization resulted into two distinct types of complexes. The Li^+ and Na^+ structures are compact and stabilized by additional interactions of the carbonyl oxygen of a monomer with the partly acidic H atoms of the CH bond of a neighboring monomer. The K^+– C^+ structures are open structures in which such bonds are no longer present. The first type of structure is unlikely to occur in proteins, since the CH bond is replaced by a CC bond of the peptide backbone. We did not search for alternatives to it, since we are interested at this stage in the validation of the SIBFA interaction energies with respect to QC for diverse arrangements. The least agreement between ΔE(SIBFA) and ΔE(QC) is for the Na^+ complex, where ΔE(SIBFA) overestimates ΔE(QC) by 6%, while the agreement for the four other complexes is < 5%.

Hexamers. The search was limited to the Na^+ – Cs^+ series because the small size of Li^+ prevents it from binding to six ligands of the size of formamide. The structures of the four energy-minimized complexes are represented in Figures 9(a-d) and the results are reported in Table VIII. Relative to the tetraformamide–Na^+ complex, the ΔE(SIBFA) error of the hexaligated complex is reduced from 6 to 3.8%, comparable to that in the Cs^+ complex, while the K^+ and Rb^+ complexes have relative errors < 1%. The overall agreement is very encouraging in view of simulations of large systems such as ion channels or macrocyclic ligands, where due to covalent attachment of

For Peer Review

the ligands, the binding distances to the cations would elongate and thus further reduce the errors.

The actual magnitude of E_{pol} in the mono- versus oligoligated complexes of the metal cations is governed by non-additivity. The anticooperativity of E_{pol} in the polyligated complexes of the metal cations can be exemplified in the case of the complex of Na+ with n=1, 4, and 6 formamide ligands. Thus E_{pol} amounts to -10 kcal/mol out of -40 for n=1, to -19 out of -100 kcal/mol for n=4, and to -14 out of -127 kcal/mol for n=6. This represents progressive decreases of its contribution to ΔE, from 25 to 11%. E_{pol}(SIBFA) is confirmed to quantitatively account for such trends. Related validations were previously reported for the Zn(II) divalent cation [27, 61] Such reductions should by no means be taken as an indication that E_{pol} could be discarded in polyligated complexes. Indeed, there is a different outcome in the case of multiply hydrogen-bonded water [62] and N-methylformamide molecules [63], which are strongly cooperative. In such complexes E_{pol} non-linearly increases in magnitude upon increasing the number of ligands, its values being larger than its summed values in all the binary complexes considered individuallly. A complex interplay of cooperativity and anticooperativity comes into play in metalloproteins, such as superoxide dismutase (SOD) which has a bimetallic core on the one hand, and on the other hand a dense water network in its vicinity. In a recent study on this protein [64], we thus found the sum of on the other hand E_{pol} and E_{ct} to account for about 35% of ΔE(HF). Such an interplay can be anticipated in ionic channels as well. In these water networks are at the entrance of the cation selectivity filters, while the permeating cations are connected to monodimensional water networks which traverse the channel [14-16].

The validations reported in the present work relied on energy-decomposition analyses but did not extend beyond n=6 ligands because with the aug-cc-pVTZ(-f) basis set, such analyses would become compute-prohibitive. However, validation of SIBFA with respect to QC calculations have been reported on complexes of the recognition sites in metalloenzymes [65, 66], which could encompass up to 300 atoms [64]. The relative errors of ΔE(SIBFA) with respect to ΔE(QC) were limited to <3%.

Impact of correlation on the binding energies and their contributions

B3LYP single-point computations were done on all four O-ligands, one N-ligand, imidazole, and one S-ligand, methanethiolate, at the HF equilibrium distance. The results are reported in

For Peer Review

Supporting Information S1a-S1e. Inclusion of correlation brings about very limited changes in the magnitude of ΔE with respect to the HF values. This appears consistent with a similar outcome found in the Li^+ – Cs^+ series in their mono- and polyhydrated complexes with coordination number *n* varying from 1 to 6, upon comparing HF and MP2 results [67]. This was also found for two alkaline-earth cations, Mg(II) and Ca(II). In contrast, ΔE in the closed-shell transition metal cations, Zn(II) and Cd(II), had a significant contribution from correlation/dispersion [66]. However, as shown by the CSOV analysis (see Methods), such a near-equivalence of ΔE(B3LYP) and ΔE(HF) stems from a compensation of effects: there is a lowering of the magnitude of EC concomitant with an increase in the magnitude of E_{pol}. These features were previously noted upon comparing the CSOV analyses done at the HF and B3LYP levels [68]. The two-short range contributions, E_{exch} and E_{ct}, retain values similar to those in the HF computations except those for formate complexes, where E_{exch} and E_{pol} both increase by a factor of app. 2. Due to the use of correlated multipoles and polarizabilities, ΔE(SIBFA) can match closely ΔE(B3LYP), except, again in the case of the formate complexes. Although the polarizabilities derived from the correlated molecular orbitals are larger than those derived from the HF ones, they are not large enough to double the E_{pol} values. We have verified that reducing the values of the two parameters used for the screening does not help to match the behavior of E_{pol}. For these formate complexes, E_{rep}(SIBFA), which in its expression embodies dependences upon the atomic charges, also increases upon passing to the correlated level, but much less so than EX. The limited increases in magnitude of E_{pol} and E_{rep} with respect to their correlated density functional counterparts appear to compensate one another to some extent.

For Peer Review

Discussion and Perspectives

Grounded on ab initio QC calculations with the aug-cc-pVTZ(-f) basis set, we have calibrated five alkali cations in the Li^+–Cs^+ series in the context of the SIBFA procedure. This is motivated by the important roles that these cations exert in the regulation of numerous biological processes, in supramolecular and bioinorganic chemistry, and in materials science. The general parameters

used to reproduce aug-cc-pVTZ(-f) basis set calculations were recently derived [39] with the I-NoLLS procedure [41, 42]. A limited amount of additional calibration was necessary for each cation, involving only cation parameters. It concerned their complexes with a small subset of ligands: water, imidazole, methanethiolate and selenothiolate for O-, N-, S-, and Se-containing ligands, respectively. Close agreements could be obtained, in most cases, for the total interaction energies and their individual contributions. Since along this series, the highest filled cation molecular orbitals are essentially of spherical symmetry, it was the smallest cation that was the most difficult to represent, namely Li^+, as it has the shortest interatomic equilibrium distances. Specifically, the largest errors were found for the Li^+–formamide complex. Overall, two ligands appeared less satisfactory than the others: trimethylamine and selenothiolate. For both, the agreement in terms of ⍰E was due to an overestimated E_{rep}(SIBFA) with a concomitant overestimation of E_{pol}. For selenothiolate, E_{ct} was overestimated by SIBFA in its complexes with the largest two cations, Rb^+ and Cs^+.

Since binding of the alkali cations occurs predominantly with O-ligands, we further validated the procedure by considering tetra- and hexaligated complexes with two of their most common ligands, namely water and formamide. For the $M^+[H_2O]_4$ complexes, the SIBFA calculations accounted accurately for the QC preference favoring the pyramidal arrangement over the planar one for small cations (Li^+ and Na^+), imposed by both first-order E_1 and second-order E_2 contributions. Such a preference diminished regularly upon increasing the size of the cation. For the $M^+[H_2O]_6$ complexes, they accounted correctly for a small but notable preference in favor of a trigonal bipyramidal arrangement over the octahedral one, which gradually sets in upon progressing along the Li^+ – Cs^+ series. Remarkably, for the Rb^+ and Cs^+ complexes, such a preference was due to E_2 counteracted by E_1, in marked contrast with the situation with the tetrahydrates. Within E_2, another noteworthy feature appeared concerning a possible emerging weight of E_{ct} in favoring the bipyramidal complex over the octahedral one, even though E_{ct} is insignificant in the monohydrated complexes except Li^+. It is due to the onset of the three H-bonds, which stabilize each of the two cyclic water trimers of the bipyramidal complex. Overall such results indicate that the selective recognition of one cation in the series compared to the others could not be simply reduced to 'size-selectivity' at play in the balance between cation-receptor complexation energy and cation desolvation energy, as this would be limited to first-order electrostatic and van der Waals interactions, namely repulsion and dispersion. Thus the

For Peer Review

results on the hexahydrates highlight the impact of second-order effects, which could overcome the preferences set by the first-order contributions, and the need for a separable formulation of the energy embodying an explicit charge-transfer contribution.

The other polyligated complexes considered have the cation bound to four or six formamides. Each SIBFA contribution could reproduce closely its QC counterpart, and the total interaction energies reproduced the corresponding QC ones with errors <6%. The energy-minimized hexaligated structures, which are less compact around the cations, show better agreement with the QC energies, as the relative errors in total energies is now < 4%. Closer agreement could even be anticipated in large molecular complexes such as macromolecules or macrocyclic hosts since in these, the cation-binding ligands are anchored to the entity they belong to by covalent bonds restricting their mobilities.

We have also evaluated the impact of electron correlation on the interaction energies and their contributions. In marked contrast with transition metal cations, correlation had a minor impact on the total interaction energies, akin to earlier results obtained for the alkaline-earth cations Mg(II) and Ca(II) [66. We observed a mutual compensation by a reduction in the magnitude of the first-order electrostatic energy concomitant with an increase in the magnitude of the second-order polarization energy. Both trends were previously shown for H-bonded complexes and the complexes of ligands with metal cations including transition metal cations [68].

Extension of this work will be two-fold. We plan to address selectivity issues at the entrance of ion channels. An issue that has yet to be addressed in detail relates to quantifying the impact of the separate contributions and of many-body effects at play in the selectivity filter, which involve cation-bound waters or water networks. Such effects were previously analyzed by QC and SIBFA computations for both cation-ligand complexes [61] and water clusters [62]. The SIBFA analyses could be paralleled and validated by QC computations on models extracted from the larger molecular complexes, as was reported previously for ligand-macromolecule complexes [65, 66]. We also plan, using Monte-Carlo approaches, to resume simulations on the complexes of these cations with macromolecular hosts to try and unravel the determinants of selectivity. We would thus expand on a much larger scale the studies with this polarizable potential, which were initiated in the early eighties. These prospects should be considerably facilitated by novel, highly

For Peer Review

scalable procedures to compute the second-order contributions [69; and Narth et al., manuscript in preparation].

Appendix. Values of the effective radii of the M+ cations and of the pairwise atom-dependent multiplicative constants.

Acknowledgments.

We thank the Grand Equipement National de Calcul Intensif (GENCI): Institut du Développement et des Ressources en Informatique Scientifique (IDRIS), Centre Informatique de l'Enseignement Supérieur (CINES), France, project No. x2009-075009), and the Centre de Ressources Informatiques de Haute Normandie (CRIHAN, Rouen, France), project 1998053. We are grateful for support from Academia Sinica and the Ministry of Science & Technology, Taiwan. T.D. is supported by the Institute of Biomedical Sciences at Academia Sinica and EU Grant "Beyond Everest", FP7-REGPOT-2011-1". Work in Basel us financially supported by the Swiss National Science Foundation through the NCCR-MUST and the University of Basel.

For Peer Review

References.

1) F. Marmol, *Progr. Neuro-Psychopharmacol. Biol. Psychiatry,* **2008,** *32,* 1761.

2) D. Meffre, J. Grenier, S. Bernard, S. Courtin, T. Dudev, G. Schakleford, M. Jafarian-Teherani, C. Massaad, *Cell. Mol. Life Sci.,* **2014***, 71*, 1123.

3) T. Dudev, C. Lim, *J. Am. Chem. Soc.* **2011***, 133,* 9506.

4) C. Maffeo, S. Bhattacharya, J. Yoo, D. Wells, A. Aksimentiev, *Chem. Rev.* **2012***, 112*, 6250

5) D. Lemoine, R. Jiang, A. Taly, T. Chataigneau, A. Specht, T. Grutter, *Chem. Rev.* **2012***, 112*, 6285.

6) L. Sauguet, F. Poitevin, S. Murail, C. van Renterghem, G. Moraga-Cid, L. Malherbe, A. W. Thompson; P. Koehl, P.-J. Corringer, M. Baaden, *EMBO J.,* **2013,** *32,* 728.

7) B. Hille, Ion *Channels of Excitable Membranes*; 3rd ed.; Sinauer Associates: Sunderland, MA, 2001.

8) M. Cavallari, A. Calzolari, A. Garbesi, R. Di Felice *J. Phys. Chem. B.* **2006***, 110,* 26337.

9) J. Sponer, A. Mladek, N. Spackova, X. Cang, T. E. Cheatham III, S. Grimme, *J. Am. Chem. Soc.* **2013***, 135,* 9785.

10) M. Rajkovski, J. Plavec, *J. Phys. Chem. C* **2012,** *116,* 23821.

11) C. J. Anderson, M. J. Welch, *Chem. Rev.* **1999,** *99*, 2219.

12) *Radioactive waste management and disposal,* Ed. L. Cecille, Elsevier, New York, 1991.

13) A. S. Relman, *Yale J. Biol. Med.* **1956,** *29, 248.*

14) (a) M. S. Prevost, L. Sauguet, H. Nury, C. van Renterghem, C. Huon, F. Poitevin, M. Baaden, M. Delarue, P.-J. Corringer, *Nature Struct. Mol. Biol.* **2012***, 19*, 642; (b) L. Sauguet, F. Poitevin, S. Murail, C. van Renterghem, G. Moraga-Cid, L. Malherbe, A. W. Thompson, P. Koehl, P.-J. Corringer, M. Baaden, M. Delarue. *EMBO J,* ***2013,*** 1.

15) X. Tao, J. Avalos, R. MacKinnon, *Science* **2009**, *326,* 1668.

16) A. N. Thompson, I. Kim, T. D. Panisian, T. M. Iverson, T. W. Allen, C. N. Nimigean, *Nature Struct. Mol. Biol.* **2009,** *16*, 1317.

17) P. Schmitt, P. D. Beer, M. G. B. Drew, P. D. Sheen, *Angew. Chem. Int. Ed.* **1997,** *36,* 1840.

For Peer Review

18) S. E. Matthews, P. Schmitt, V. Felix, M. G. B. Drew, P. D. Beer, *J. Am. Chem. Soc.,* **2002,** *124*, 1341.

19) W. Sliwa, T. Girek, *J. Incl. Phenom. Macrocycl. Chem.* **2010***, 66,* 15.

20) T. Dudev, C. Lim, *J. Am. Chem. Soc.,* **2009***, 131*, 8092.

21) (a) T. Dudev, C. Lim, *J. Am. Chem. Soc.,* **2010***, 132***,** 2321. (b) T. Dudev, C. Lim, *Acc. Chem. Res.* **2014,** DOI: 10.1021/ar5002878

22) (a) G. Lamoureux, E. Harder, I. V. Vorobyov, B. Roux, A. D. MacKerell, *Chem. Phys. Letts.* **2006***, 418,* 245; (b) E. Harder, V. M. Anisimov, I. V. Vorobyov, P. E. M. Lopez, S. Y. Noskov, A. D. MacKerell, *J. Chem. Theory Comput.* **2006,** *2,* 1587; (c) H. Yu, T. W. Whitfield, E. Harder, G. Lamoureux, I. Vorobyov, V. M. Anisimov, A. D. MacKerell Jr., B Roux, *J. Chem. Theory Comput.* **2010***, 6*, 774; (d) C. M. Baker, P. E. M. Lopez, X. Zhu, B. Roux, A. D. MacKerell, *J. Chem. Theory Comput.* **2010***, 6,* 1181.

23) Roux, B.; Berneche, S.; Egwolf, B.; Lev, B.; Noskov, S. Y.; Rowley, C. N.; Yu, H. *J. Gen. Physiol.* **2011***, 137,* 415, and refs. therein.

24) N. Gresh, A. G. Cisneros, T. A. Darden, J.-P. Piquemal *J. Chem. Theory Comput.* **2007**, *3*, 1960.

25) M. D. Tissandier, K. A. Cohen, W. Y. Feng, E. Gundlach, M. H. Cohen, A. D. Earhart, J. V. Coe, T. R. Tuttle Jr., *J. Phys. Chem. A* **1998***, 102*, 7787.

26) N. Gresh, D. R. Garmer, *J. Comput. Chem.* **1996,** *17,* 1481.

27) (a) N. Gresh, *J. Comput. Chem.* **1995,** *16,* 856; (b) N. Gresh, J.-P. Piquemal, M. Krauss, M. *J. Comput. Chem.,* **2005***, 26,* 1113.

28) N. Gresh, C. Policar, C. Giessner-Prettre, *J. Phys. Chem. A,* **2002**, *106*, 5660.

29) J.-P. Piquemal, B. W. Hubbard, N. Fey, R. Deeth, N. Gresh, C. Giessner-Prettre, *J. Comput. Chem.* **2003**, *24,* 1963.

30) M. Devereux, M.-C. van Severen, O. Parisel, J.-P. Piquemal, N. Gresh, *J. Chem. Theory Comput.* **2011***, 7,* 138.

31) R. Chaudret, N. Gresh, O. Parisel, J.-P. Piquemal, *J. Comput. Chem.* **2011***, 31*, 2949.

For Peer Review

32) A. Marjolin, C. Gourlaouen, C. Clavaguéra, P. Ren, J. Wu, N. Gresh, J.-P. Dognon, J-P. Piquemal, *Theor. Chem. Acc.,* **2012,** *131*, 1199.

33) (a) N. Gresh, P. Claverie, A. Pullman, A. *Int. J. Quantum Chem. Symp* **1979,** 13, 243; (b) N. Gresh, A. Pullman, P. Claverie, *Int. J. Quantum Chem.* **1985,** *28,* 757.

34) N. Gresh, C. Etchebest, O. de la Luz Rojas, A. Pullman, *Int. J. Quantum Chem.* Quantum Biol. Symp. **1981**, *1*, 109.

35) N. Gresh, A. Pullman, *Int. J. Quantum Chem*. **1982**, *22*, 709.

36) N. Gresh, A. Pullman, *New J. Chem.* **1986,** *10*, 405.

37) C. Etchebest, A. Pullman, (a) *FEBS Letts.* **1983***, 163,* 199; (b) *FEBS Letts.* **1984,** *170,* 191*;* (c) *FEBS Letts.* **1984***, 173,* 301.

38) N. Gresh, B. Pullman, *Int. J. Quantum Chem.*, *Quantum Biol. Symp.* **1986**, *12,* 49.

39) M. Devereux, N. Gresh, J.-P. Piquemal, M. Meuwly, *J. Comput. Chem.,* **2014,** *35,* 1577.

40) G. Kuppuraj, M. Dudev, C. Lim, *J. Phys. Chem. B* **2009,** 113, 2952.

41) M. M. Law, J. M. Hutson, *Comp. Phys. Comm.* **1997***, 102,* 252.

42) M. Devereux, M. Meuwly, *J. Chem. Inf. Model.,* **2010***, 50,* 349.

43) W. J. Stevens, W. Fink, *Chem. Phys. Letts.* **1987,** *139,* 15.

44) (a) S. F. Boys, F. Bernardi, *Mol. Phys.* **1970**, *19*, 553; (b) S. Simon, M. Duran, J. J. Dannenberg, *J. Chem. Phys.* **1996**, *105*, 11024.

45) M. W. Schmidt, K. K. Baldridge, J. A. Boatz, S. T. Elbert, M. S. Gordon, J. H. Jensen, S. Koseki, N. Matsunaga, K. A. Nguyen, S. Su, T. L. Windus, M. Dupuis, J. A. Montgomery, *J. Comput. Chem.* **1993,** *14,* 1347.

46) (a) T. H. Dunning, *J. Chem. Phys.* **1989**, *90*, 1007; (b) D. Feller, *J. Comput. Chem.* **1996***, 17*, 1571.

47) (a) A. D. Becke, *Phys. Rev. A* **1988***, 38,* 3098; (b) A. D. Becke, *J. Chem. Phys.* **1993***, 98,* 1372; (c) A. D. Becke, *J. Chem. Phys.* **1993,** *98,* 5648; (d) C. Lee, W. Yang, R. G. Parr, *Phys. Rev. A,* **1988***, 37*, 785..

48) P. S. Bagus, K. Hermann, C. Bauschlicher, *J. Chem. Phys.* **1984,** *80,* 4378.

49) M. Dupuis, A. Marquez, E. R. Davidson, Hondo95.3, QCPE Bloomington, IN.

50) A. Bergner, M. Dolg, W. Kuechle, H. Stoll, H. Preuss, *Mol. Phys.* **1993***, 80,* 1431.

51) J. P. Piquemal, N. Gresh, C. Giessner-Prettre, *J. Phys. Chem. A.,* **2003***, 107,* 10353.

52) (a) A. J. Stone, *Chem. Phys. Letts.* **1981,** *83,* 233; (b) A. J. Stone, M. Alderton, *Mol. Phys.* **1985**, *56*, 1047; (c) A. J. Stone, *J. Chem. Theory Comput.* **2005***, 1,* 1128.

53) F. Vigné-Maeder, P. Claverie, *J Chem Phys* **1988**, *88,* 4934.

54) C. Kramer, T. Bereau, A. Spinn, K. R. Liedl, P. Gedeck, M. Meuwly, *J. Chem. Inf. Model.,* **2013***, 53*, 3410.

55) D. R. Garmer, W. J. Stevens, *J Phys Chem* **1989**, *93*, 8263.

56) J. A. Evangelakis, J. P. Rizos, I. E. Lagaris, I. N. Demetropoulos, *Comput. Phys. Commun.* **1987***, 46,* 401.

57) E. D. Glendening, W. Feller, *J. Phys. Chem.* **1995**, *99,* 3060.

58) (a) P. Kebarle, *Ann. Rev. Phys. Chem.* **1977,** *28*, 445;(b) M. A. Duncan, *Int. J. Mass Spectrom.* **2000**, *200,* 545.

59) D. J. Miller, M. Lisy, *J. Am. Chem. Soc.* **2008,** *130*, 15381.

60) (a) L. Rulisek, Z. Havlas, *J. Am. Chem. Soc.* **2000,** *122,* 10428; (b) L. Rulisek, Z. Havlas, *J. Phys. Chem. A* **2002***, 106,* 3855; (c) L. Rulisek, Z. Havlas, *J. Phys. Chem. B* **2003***, 107*, 2376; (d) O. Gutten, I. Besseova, L. Rulisek, *J. Phys. Chem. A* **2011***, 115,* 11394.

61) G. Tiraboschi, N. Gresh, C. Giessner-Prettre, L. G. Pedersen, D. W. Deerfield, *J Comput Chem* **2000,** *21*, 1011.

62) (a) N. Gresh, *J. Phys. Chem. A* **1997***, 101,* 8690; (b) M. Masella, N. Gresh, J., J.-P. Flament, *J. Chem. Soc. Faraday,* **1998***, 94,* 2745; (c) J.-P. Piquemal, R. Chelli, P. Procacci, N. Gresh, *J. Phys. Chem. A,* **2007,** *111,* 8170.

63) H. Guo, N. Gresh, B.-P. Roques, D. S. Salahub, *J. Phys. Chem. B,* **2000,** *104,* 9746.

64) N. Gresh, K. El Hage, D. Perahia, J.-P. Piquemal, C. Berthomieu, D. Berthomieu, *J. Comput. Chem.* **2014***, 35*, 2096

65) N. Gresh, N. Audiffren, M. Ledecq, J. de Ruyck, J. Wouters, *J. Phys. Chem. B* **2010***, 114,* 4885.

66) N. Gresh, B. de Courcy, J.-P. Piquemal, J. Foret, S. Courtiol-Legourd, L. Salmon, *J. Phys. Chem. B* **2011,** *115,* 8304.

67) D. R. Garmer, N. Gresh, *J. Am. Chem. Soc.,* **1994***, 116,* 8556.

68) J.-P. Piquemal, A. Marquez, O. Parisel, C. Giessner-Prettre, *J. Comput. Chem.* **2005***, 26,* 1052.

69) F. Lipparini, L. Lagardère, B. Stamm, E. Cances, M. E. Schnieders, P. Ren, Y. Maday, J.-P. Piquemal, *J. Chem. Theory Comput.* **2014**, *10,* 1638.

The actual magnitu

For Peer Review

Figure captions

Figure 1. Li^+ – H_2O complex. Compared evolutions of ΔE(QC) and ΔE(SIBFA) and of their contributions upon variations of the Li^+ – O distance.

Figure 2. Na^+ – formate complex. Compared evolutions of ΔE(QC) and ΔE(SIBFA) and of their contributions upon variations of the Na^+ – O distance. a) bidentate binding. b) monodentate binding formate complex.

Figure 3. K^+ – formamide complex. Compared evolutions of ΔE(QC) and ΔE(SIBFA) and of their contributions upon variations of the K^+– O distance.

Figure 4. Rb^+ – imidazole complex. Compared evolutions of ΔE(QC) and ΔE(SIBFA) and of their contributions upon variations of the Rb^+ – N distance.

Figure 5. Cs^+ – methanethiolate complex. Compared evolutions of ΔE(QC) and ΔE(SIBFA) and of their contributions upon variations of the Cs^+ – S distance.

Figure 6. Polycoordinated complex of Li^+ with four water molecules. a) Square-planar; b) pyramidal.

Figure 7. Polycoordinated complex of Cs^+ with six water molecules. a) octahedral; b) bis-pyramidal.

Figure 8. Tetracoordinated complexes of formamide with a) Li^+; b) Na^+; c) K^+; d) Rb^+; and e) Cs^+.

Figure 9. Hexacoordinated complexes of formamide with a) Na^+; b) K^+; c) Rb^+; and d) Cs^+.

Supporting Information. Monoligated Li^+ – Cs^+ complexes. Values of the correlated QC and SIBFA interaction energies and their contributions.

For Peer Review

Appendix

Values of the atom-type dependent pairwise K multiplicative constants

	H	C	N	O	S	Se
Li+	8.68	8.68	10.51	10.78	11	4
Na+	25.87	25.87	31.5	32.1	11	11
K+	59.3	59.3	72.1	73.5	54.9	21.6
Cs+	72.8	72.8	74.2	99	82.8	8.8

Values of the effective radii

	W(rep)	W(pol)	W(ct)	W(Epen)
Li+	1.15	1.78	1.26	1.02
Na+	1.22	1.98	1.22	0.78
K+	1.38	1.98	1.48	1.17
Rb+	1.43	1.98	1.78	1.47
Cs+	1.48	2.03	1.88	1.69

Review

Table I. Monoligated Li+ complexes. Values (kcal/mol) of the QC and SIBFA interaction energies and their contributions.

Oxygen ligands

	H2O, d=1.80		Formamide, d=1.70		Methanol, d=1.80		Formate bridge, d=2.10		Formate external, d=1.70	
	QC	SIBFA	QC	SIBFA	QC	SIBFA	QC	SIBFA	QC	SIBFA
EC/EMTP*	-36.1	-36.1	-51.4	-48.5	-36.9	-35.9	-174.9	-166.1	-156.9	-146.5
Eexch/Erep	14.2	14.3	18.6	21	15.3	14.6	26.8	27.4	33.2	26.9
E1	-21.9	-21.8	-32.8	-27.5	-21.5	-21.3	-148.1	-138.7	-123.7	-119.6
Epol	-10.8	-10.9	-18.5	-18.7	-14.9	-12.9	-21	-22.6	-17.9	-19.6
Ect	-2.3	-1.9	-3	-1.6	-3.4	-1.9	-3.7	-5.1	-5.2	-5.1
DE	**-34.9**	**-34.5**	**-54.4**	**-47.9**	**-37.2**	**-36.2**	**-172.9**	**-166.3**	**-146.9**	**-144.4**

Nitrogen and sulfur ligands

	imidazole, d=1.90		Pyridine, d=1.90		Trimethylamine, d=1.90		Methanethiolate, d=2.20 A		Methionine, d=2.40 A	
	QC	SIBFA	QC	SIBFA	QC	SIBFA	QC	SIBFA	QC	SIBFA
EC/EMTP*	-49.8	-48.9	-44.1	-40.4	-44.5	-39.4	-154.9	-155.6	-15.9	-14.4
Eexch/Erep	19.6	17.4	20.5	18.3	24.4	21.2	30.1	27.7	9.5	10.6
E1	-30.2	-31.5	-23.6	-22.2	-20	-18.2	-124.8	-127.9	-6.4	-3.8
Epol	-17.8	-20.2	-19.5	-21.1	-18.8	-22.3	-20	-29.4	-29.4	-23.1
Ect	-3.4	-2.9	-3.4	-3.1	-3.4	-2.5	-6.8	-3.5	-3.3	-2.3
DE	**-51.3**	**-54.6**	**-46.6**	**-46.3**	**-42.4**	**-42.9**	**-151.7**	**-160.8**	**-28.3**	**-29.4**

Selenium ligands

	selenocysteinate, d=2.30		Selenomethionine, d=2.4 A	
	QC	SIBFA	QC	SIBFA
EC/EMTP*	-142.6	-150.3	-15.9	-14.4
Eexch/Erep	23.1	27.5	9.5	10.6
E1	-119.5	-122.8	-6.4	-3.9
Epol	-19.9	-34	-18.5	-23.1
Ect	-7.1	-7.2	-3.3	-2.4
DE	**-146.5**	**-164**	**-28.3**	**-29.4**

For Peer Review

Table II. Monoligated Na+ complexes. Values (kcal/mol) of the QC and SIBFA interaction energies and their contributions.

Oxygen ligands

	H2O, d=2.20		Formamide, d=2.10		Methanol, d=2.20		Formate bridge, d=2.50		Formate external, d=2.10	
	QC	SIBFA	QC	SIBFA	QC	SIBFA	QC	SIBFA	QC	SIBFA
EC/EMTP*	-26.9	-27.6	-40.6	-41.8	-27.1	-28	-158.6	-155.5	-133.4	-130.1
Eexch/Erep	8.8	9.2	11.7	13.3	9.6	9.4	24.4	22	22.5	15.8
E1	-18	-18.4	-28.8	-28.6	-17.5	-18.6	-134.2	-133.5	-110.9	-114.4
Epol	-5.6	-5.6	-10	-10.1	-7.2	-6.9	-11.8	-10.8	-9.8	-9.3
Ect	-0.1	-0.1	-0.1	-0.1	-0.1	-0.1	-0.4	-0.3	-0.4	-0.3
DE	**-23.8**	**-24.1**	**-39.1**	**-38.7**	**-24.9**	**-25.5**	**-146.5**	**-144.6**	**-121.2**	**-123.9**

Nitrogen and sulfur ligands

	imidazole, d=2.30		Pyridine, d=2.40		Trimethylamine, d=2.40		Methanethiolate, d=2.50 A		Methionine, d=2.70 A	
	QC	SIBFA	QC	SIBFA	QC	SIBFA	QC	SIBFA	QC	SIBFA
EC/EMTP*	-37.9	-38.7	-29.4	-28	-28.7	-32.2	-146	-138.5	-17	-15.9
Eexch/Erep	13.1	12.7	9.5	9.1	11.9	12.8	32	27.4	7.1	8.2
E1	-24.8	-26	-19.9	-18.8	-16.9	-19.5	-114	-111.1	-10	-7.7
Epol	-9.7	-11.4	-10.8	-10.7	-10.2	-12.3	-13.3	-18.3	-10.6	-12.9
Ect	-0.2	-0.1	-0.2	-0.1	-0.2	-0.1	-1.3	-0.3	-0.3	0
DE	**-35.6**	**-37.5**	**-31**	**-29.6**	**-27.4**	**-31.8**	**-128.8**	**-129.7**	**-20.9**	**-20.7**

Selenium ligands

	selenocysteinate, d=2.60		Selenomethionine, d=2.80 A	
	QC	SIBFA	QC	SIBFA
EC/EMTP*	-140.7	-136.1	-14.3	-15.4
Eexch/Erep	31.7	29.6	6.8	7.8
E1	-109	-106.5	-7.5	-7.6
Epol	-14.4	-21.3	-11.3	-13.4
Ect	-1.7	-0.6	-0.5	-0.1
DE	**-125.2**	**-128.4**	**-19.3**	**-21.2**

For Peer Review

Table III. Monoligated K+ complexes. Values (kcal/mol) of the QC and SIBFA interaction energies and their contributions.

Oxygen ligands

	H2O, d=2.70		Formamide, d=2.60		Methanol, d=2.70		Formate bridge, d=2.90		Formate external, d=2.40	
	QC	SIBFA	QC	SIBFA	QC	SIBFA	QC	SIBFA	QC	SIBFA
EC/EMTP*	-18.1	-17.7	-28.9	-28.2	-17.8	-17.3	-138	-130.4	-117.4	-110.1
Eexch/Erep	4.9	5.1	6.4	6.9	5.3	5.3	23.7	19.5	24.2	18
E1	-13.1	-12.7	-22.5	-21.3	-12.5	-12	-114.3	-110.9	-93.2	-92.1
Epol	-3	-3.3	-5.6	-6.3	-4	-4.3	-8.2	-9.2	-7.5	-8.1
Ect	-0.2	-0.2	-0.3	-0.2	-0.2	-0.3	-1.5	-1.3	-1.3	-1.2
DE	**-16.3**	**-16.3**	**-28.6**	**-27.8**	**-16.7**	**-16.6**	**-124.2**	**-121.4**	**-102.7**	**-101.4**

Nitrogen and sulfur ligands

	imidazole, d=2.80		Pyridine, d=2.80		Trimethylamine, d=2.90		Methanethiolate, d=3.00 A		Methionine, d=3.20 A	
	QC	SIBFA	QC	SIBFA	QC	SIBFA	QC	SIBFA	QC	SIBFA
EC/EMTP*	-25.5	-25	-21.1	-19	-17.6	-20.3	-117.9	-110.1	-12.2	-13.7
Eexch/Erep	7.5	7.4	7.8	7.8	6.9	12	21.4	17.5	4.5	5
E1	-17.9	-17.6	-13.3	-11.3	-10.7	-8.3	-96.5	-92.7	-7.7	-6.7
Epol	-6	-7.3	-6.8	-7.1	-6	-8.6	-7.7	-12.4	-5.8	-7.7
Ect	-0.5	-0.2	-0.4	-0.3	-0.3	-0.2	-2.1	-1	-0.3	-0.1
DE	**-24.5**	**-25.2**	**-20.7**	**-18.6**	**-17.1**	**-17.2**	**-106.4**	**-106.1**	**-13.9**	**-16.4**

Selenium ligands

	selenocysteinate, d=3.10		Selenomethionine, d=3.40 A	
	QC	SIBFA	QC	SIBFA
EC/EMTP*	-114.6	-107.6	-9.9	-8.5
Eexch/Erep	22	21.6	3.3	3.4
E1	-92.6	-86	-6.6	-5
Epol	-8.2	-14.6	-5.9	-7.4
Ect	-2.3	-2.7	-0.3	-0.3
DE	**-103.1**	**-103.3**	**-12.7**	**-12.7**

For Peer Review

Table IV. Monoligated Rb+ complexes. Values (kcal/mol) of the QC and SIBFA interaction energies and their contributions.

Oxygen ligands

	H2O, d=2.90		Formamide, d=2.70		Methanol, d=2.90		Formate bridge, d=3.10		Formate external, d=2.60	
	QC	SIBFA	QC	SIBFA	QC	SIBFA	QC	SIBFA	QC	SIBFA
EC/EMTP*	-15.8	-15.9	-27.7	-27.6	-15.5	-15.5	-129.2	-122.2	-108.5	-102.1
Eexch/Erep	4.2	4.3	7.9	7.7	4.5	4.7	21.2	16.9	19.8	17.2
E1	-11.6	-11.6	-19.8	-19.9	-10.9	-10.8	-108	-105.3	-88.8	-85
Epol	-2.4	-2.7	-5.2	-5.6	-3.2	-3.5	-7.4	-7.6	-6.7	-6.7
Ect	-0.2	-0.2	-0.5	-0.5	-0.2	0	-2.1	-1.9	-2	-1.8
DE	**-14.2**	**-14.5**	**-25.7**	**-26**	**-14.5**	**-14.3**	**-117.7**	**-114.7**	**-97.7**	**-93.5**

Nitrogen and sulfur ligands

	imidazole, d=3.00		Pyridine, d=3.00		Trimethylamine, d=3.00		Methanethiolate, d=3.10 A		Methionine, d=3.40 A	
	QC	SIBFA	QC	SIBFA	QC	SIBFA	QC	SIBFA	QC	SIBFA
EC/EMTP*	-22.2	-22.1	-18.3	-16.7	-16.6	-17.2	-114.5	-106.8	-10.9	-9.5
Eexch/Erep	6.4	6.2	6.6	2.9	8.1	12.4	24.2	20.7	3.9	4.2
E1	-15.9	-15.9	-11.6	-13.8	-8.5	-4.7	-90.3	-86.2	-7	-5.3
Epol	-5.1	-6	-5.8	-5.8	-5.6	-7.1	-7.6	-11.3	-4.8	-6.2
Ect	-0.5	-0.2	-0.4	0	-0.5	-0.4	-2.8	-3.8	-0.3	-0.3
DE	**-21.6**	**-22.1**	**-18.1**	**-19.6**	**-14.7**	**-12.1**	**-100.9**	**-101.3**	**-12.2**	**-11.8**

Selenium ligands

	selenocysteinate, d=3.30		Selenomethionine, d=3.60 A	
	QC	SIBFA	QC	SIBFA
EC/EMTP*	-107.2	-100.7	-8.9	-7.5
Eexch/Erep	19.8	28.5	2.9	2.5
E1	-87.5	-72.2	-6	-5
Epol	-7.2	-12.2	-4.8	-6
Ect	-2.7	-8.6	-0.3	-0.3
DE	**-97.5**	**-93**	**-11.2**	**-11.4**

For Peer Review

Table V. Monoligated Cs+ complexes. Values (kcal/mol) of the QC and SIBFA interaction energies and their contributions.

Oxygen ligands

	H2O, d=3.10		Formamide, d=2.90		Methanol, d=3.2		Formate bridge, d=3.20		Formate external, d=2.70	
	QC	SIBFA	QC	SIBFA	QC	SIBFA	QC	SIBFA	QC	SIBFA
EC/EMTP*	-14.2	-14.5	-25.3	-25.3	-12.7	-12.9	-127.6	-120.5	-106.7	-100.2
Eexch/Erep	4.3	4.2	7.8	6.9	3.2	3	28.8	22.3	25.1	21.9
E1	-9.9	-10.3	-17.4	-18.4	-9.5	-9.9	-98.7	-98.3	-81.6	-78.3
Epol	-2	-2.1	-4.5	-4.6	-2.5	-2.6	-8.9	-7.6	-8.2	-6
Ect	-0.3	-0.4	-0.7	-0.5	-0.2	-0.3	-3.9	-1.9	-3.5	-2.4
DE	**-12.2**	**-12.8**	**-22.9**	**-23.5**	**-12.3**	**-12.8**	**-112**	**-107.8**	**-93.6**	**-86.8**

Nitrogen and sulfur ligands

	imidazole, d=3.10		Pyridine, d=3.20		Trimethylamine, d=3.30		Methanethiolate, d=3.30 A		Methionine, d=3.40 A	
	QC	SIBFA	QC	SIBFA	QC	SIBFA	QC	SIBFA	QC	SIBFA
EC/EMTP*	-21.6	-21.4	-16.2	-14.8	-13.1	-13.5	-106.8	-100.2	-10.9	-10.4
Eexch/Erep	8.7	8	6.5	6.7	5.7	8.9	23.3	22	3.9	7.9
E1	-12.9	-13.4	-9.7	-8.2	-7.3	-4.6	-83.5	-78.3	-7	-2.5
Epol	-5.1	-5.4	-5.1	-4.7	-4.4	-5.1	-8.3	-9.2	-4.8	-6.2
Ect	-0.8	-0.2	-0.5	-0.5	-0.5	-0.3	-3.4	-4.7	-0.3	-0.5
DE	**-19**	**-22.1**	**-15.5**	**-13.4**	**-12.4**	**-10**	**-95.4**	**-92.2**	**-12.2**	**-9.2**

Selenium ligands

	selenocysteinate, d=3.40		Selenomethionine, d=3.80 A	
	QC	SIBFA	QC	SIBFA
EC/EMTP*	-103.9	-98.9	-8.2	-7.5
Eexch/Erep	24.3	35.5	3	2.9
E1	-79.6	-63.5	-5.2	-4.6
Epol	-8.5	-11.1	-4.1	-4.8
Ect	-3.7	-12.5	-0.3	-1.1
DE	**-92**	**-87.1**	**-9.7**	**-10.6**

For Peer Review

Table VI a. Complexes of Li+ with four and six water molecules. Values (kcal/mol) of the QC and SIBFA intermolecular interactions

	[Li(H2O)4]+				[Li(H2O)6]+			
	Planar, d =2.10		Pyramidal d = 2.00		Octahedral d=2.20		Bipyramidal d=2.20	
	QC	SIBFA	QC	SIBFA	QC	SIBFA	QC	SIBFA
EC/EMTP*	-99.7	-99.2	-111	-110.6	-125.9	-125.9	-128.7	-127
Eexch/Erep	21.5	20.8	31.6	30.6	25.2	24.4	42.3	45.2
E1	-78.2	-78.3	-79.4	-80	-100.6	-101.5	-86.4	-81.8
Epol*	-18.1	-16.5	-22.3	-21.4	-14.6	-11.2	-22.3	-20.2
Epol	-15.9	-14.1	-19.4	-17.9		-12.3		-17.7
Ect	-2.5	-2.2	-4	-3.2	-0.4	-2.1	-4	-5
DE	**-96.5**	**-94.6**	**-102.6**	**-101.6**	**-115.1**	**-113.3**	**-109.6**	**-104.5**

Table VI b. Complexes of Na+ with four and six water molecules. Values (kcal/mol) of the QC and SIBFA intermolecular interactions

	[Na(H2O)4]+				[Na(H2O)6]+			
	Planar, d =2.30		Pyramidal d = 2.30		Octahedral d=2.40		Bipyramidal d=2.40	
	QC	SIBFA	QC	SIBFA	QC	SIBFA	QC	SIBFA
EC/EMTP*	-86.9	-89.6	-87.7	-90.2	-111.3	-114.1	-116.3	-119.2
Eexch/Erep	24.8	26.1	23.1	24.7	25.2	27	36.2	36.6
E1	-62.1	-63.5	-64.6	-65.5	-100.6	-87.1	-80.1	-82.6
Epol*	-11.9	-11.4	-12.7	-12.3	-10.2	-9.3	-13.6	-13.5
Epol	-11	-10.1	-11.8	-11.1	-9.1	-7.7	-12.5	-11.8
Ect	-0.3	-0.2	-0.2	-0.2	-0.4	-0.2	-1.2	-1.8
DE	**-73.2**	**-75.7**	**-76.4**	**-76.7**	**-95**	**-95.1**	**-93.4**	**-96.2**

Table VI c . Complexes of K+ with four and six water molecules. Values (kcal/mol) of the QC and SIBFA intermolecular interactions.

	[K(H2O)4]+				[K(H2O)6]+			
	Planar, d =2.80		Pyramidal d = 2.80		Octahedral d=2.90		Bipyramidal d=2.95	
	QC	SIBFA	QC	SIBFA	QC	SIBFA	QC	SIBFA
EC/EMTP*	-60.4	-59.4	-61.1	-60.1	-78.9	-77.5	-86.6	-86.3
Eexch/Erep	13.4	13.9	13.3	13.8	13.4	14.3	24.5	26.8
E1	-47	-45.4	-47.8	-46.2	-65.5	-63.2	-62.1	-59.5
Epol*	-6.9	-7.8	-7.3	-8.2	-6.4	-7.2	-9.1	-10.4
Epol		-7.2		-7.7		-6.4	-8.9	-9.8
Ect	-0.3	-0.6	-0.3	-0.6	-0.4	-0.6	-1.5	-2.4
DE	**-53.9**	**-53.3**	**-55.1**	**-54.5**	**-71.7**	**-70.2**	**-72.2**	**-71.7**

For Peer Review

Table VI d. Complexes of Rb+ with four and six water molecules. Values (kcal/mol) of the QC and SIBFA intermolecular interactions.

	[Rb(H2O)4]+				[Rb(H2O)6]+			
	Planar, d =3.00		Pyramidal d = 3.00		Octahedral d=3.00		Bipyramidal d=3.10	
	QC	SIBFA	QC	SIBFA	QC	SIBFA	QC	SIBFA
EC/EMTP*	-53.4	-53.8	-54.1	-54.5	-74.7	-75.2	-81.4	-82.7
Eexch/Erep	11.6	12.8	11.6	12.8	16.4	18.3	25.4	28.7
E1	-41.8	-41	-42.5	-41.6	-58.3	-56.9	-56	-54
Epol*	-5.7	-6.4	-5.9	-6.7	-5.9	-6.6	-9.1	-9.5
Epol		-6	-5.7	-6.4	-5.4	-5.9	-8.5	-9.2
Ect	0	-0.5	-0.4	-0.5	-0.6	-1.1	-1.6	-3
DE	**-47.6**	**-47.6**	**-48.6**	**-48.5**	**-64.3**	**-63.9**	**-66.1**	**-66.2**

Table VI e. Complexes of Cs+ with four and six water molecules. Values (kcal/mol) of the QC and SIBFA intermolecular interactions.

	[Cs(H2O)4]+				[Cs(H2O)6]+			
	Planar, d =3.20		Pyramidal d = 3.20		Octahedral d=3.20		Bipyramidal d=3.30	
	QC	SIBFA	QC	SIBFA	QC	SIBFA	QC	SIBFA
EC/EMTP	-48.3	-49.4	-48.8	-49.8	-67.4	-69.9	-76.7	-79
Eexch/Erep	12.1	11.7	12.1	11.7	16.9	16.4	28.1	29.7
E1	-36.2	-37.6	-36.7	-38.1	-50.6	-52.6	-48.6	-49.3
Epol*	-4.8	-6.4	-5.2	-5.5	-5.1	-5.5	-8.3	-9
Epol	-4.6	-5	-4.9	-5.2	-4.8	-5	-8.6	-9.1
Ect	-0.6	-1	-0.6	-1	-0.8	-1.2	-2.3	-3.5
DE	**-41.4**	**-43.6**	**-42.1**	**-44.3**	**-56.2**	**-58.8**	**-59.2**	**-61.9**

For Peer Review

Table VII. Formamide tetramers. Values (kcal/mol) of the QC and SIBFA intermolecular interaction energies and their contributions.

	Li+		Na+		K+		Rb+		Cs+	
	QC	SIBFA	QC	SIBFA	QC	SIBFA	QC	SIBFA	QC	SIBFA
EC/EMTP*	-144.9	-144.5	-130.8	-134.5	-89.9	-87.5	-81.1	-80.2	-79.6	-80.3
Eexch/Erep	39.6	36.5	51.1	45.4	16.3	17.3	13.9	13.7	19.9	17.3
E1	-105.3	-107.9	-79.7	-89.1	-73.7	-70.2	-67.3	-66.6	-59.7	-62.9
Epol*	-27.2	-25.5	-19.9	-18.8	-9.8	-11.2	-8.3	-9.5	-8	-8.3
Epol	-24	-21.5	-19.2	-17.5	-9.2	-10	-7.6	-8.6	-8.2	-7.6
Ect	-4.4	-2.6	-1.6	-0.4	-0.4	-0.5	-0.6	-0.8	-0.4	-1.1
DE	**-132.8**	**-132**	**-99.7**	**-106.7**	**-83.3**	**-80.7**	**-75.4**	**-76**	**-68.3**	**-71.6**

For Peer Review

Table VIII. Formamide hexamers. Values (kcal/mol) of the QC and SIBFA intermolecular interaction energies and their contributions

	Na+		K+		Rb+		Cs+	
	QC	SIBFA	QC	SIBFA	QC	SIBFA	QC	SIBFA
EC/EMTP*	-154.2	-158.9	-116.6	-115.9	-111.8	-112.7	-100.1	-101.8
Eexch/Erep	41	39.2	26.3	26.7	29.9	30.3	26.1	23.9
E1	-113.2	-119.7	-90.4	-89.2	-81.9	-82.4	-74	-77.9
Epol*	-13.7	-12.7	-10.3	-11.5	-9.1	-9.8	-8.6	-8.8
Epol	-13.5	-11.1	-10.6	-10.8	-9.3	-9.4	-9.3	-8.7
Ect	-1.1	-0.3	-1.3	-0.7	-1.6	-1.1	-1.3	-1.1
DE	**-126.5**	**-131.1**	**-101.5**	**-100.7**	**-92.3**	**-92.9**	**-84.6**	**-87.8**

For Peer Review

Figure captions

Figure 1. Li^+ – H_2O complex. Compared evolutions of ΔE(QC) and ΔE(SIBFA) and of their contributions upon variations of the Li^+ – O distance.

Figure 2. Na^+ – formate complex. Compared evolutions of ΔE(QC) and ΔE(SIBFA) and of their contributions upon variations of the Na^+ – O distance. a) bidentate binding. b) monodentate binding formate complex.

Figure 3. K^+ – formamide complex. Compared evolutions of ΔE(QC) and ΔE(SIBFA) and of their contributions upon variations of the K^+– O distance.

Figure 4. Rb^+ – imidazole complex. Compared evolutions of ΔE(QC) and ΔE(SIBFA) and of their contributions upon variations of the Rb^+ – N distance.

Figure 5. Cs^+ – methanethiolate complex. Compared evolutions of ΔE(QC) and ΔE(SIBFA) and of their contributions upon variations of the Cs^+ – S distance.

Figure 6. Polycoordinated complex of Li^+ with four water molecules. a) Square-planar; b) pyramidal.

Figure 7. Polycoordinated complex of Cs^+ with six water molecules. a) octahedral; b) bis-pyramidal.

Figure 8. Tetracoordinated complexes of formamide with a) Li^+; b) Na^+; c) K^+; d) Rb^+; and e) Cs^+.

Figure 9. Hexacoordinated complexes of formamide with a) Na^+; b) K^+; c) Rb^+; and d) Cs^+.

For Peer Review

e

Appendix

Values of the atom-type dependent pairwise K multiplicative constants

	H	C	N	O	S	Se
Li+	8.68	8.68	10.51	10.78	11	4
Na+	25.87	25.87	31.5	32.1	11	11
K+	59.3	59.3	72.1	73.5	54.9	21.6
Cs+	72.8	72.8	74.2	99	82.8	8.8

Values of the effective radii

	W(rep)	W(pol)	W(ct)	W(Epen)
Li+	1.15	1.78	1.26	1.02
Na+	1.22	1.98	1.22	0.78
K+	1.38	1.98	1.48	1.17
Rb+	1.43	1.98	1.78	1.47
Cs+	1.48	2.03	1.88	1.69

Review

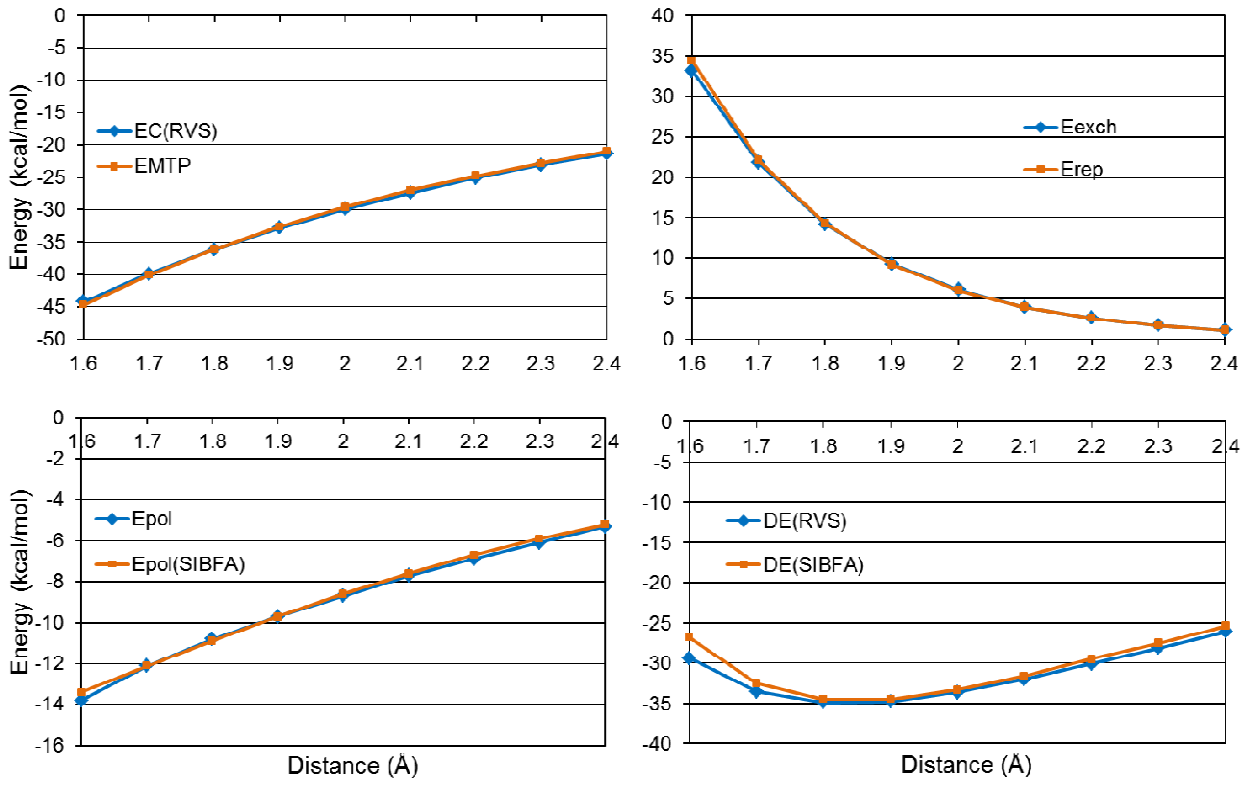

Figure 1

er Review

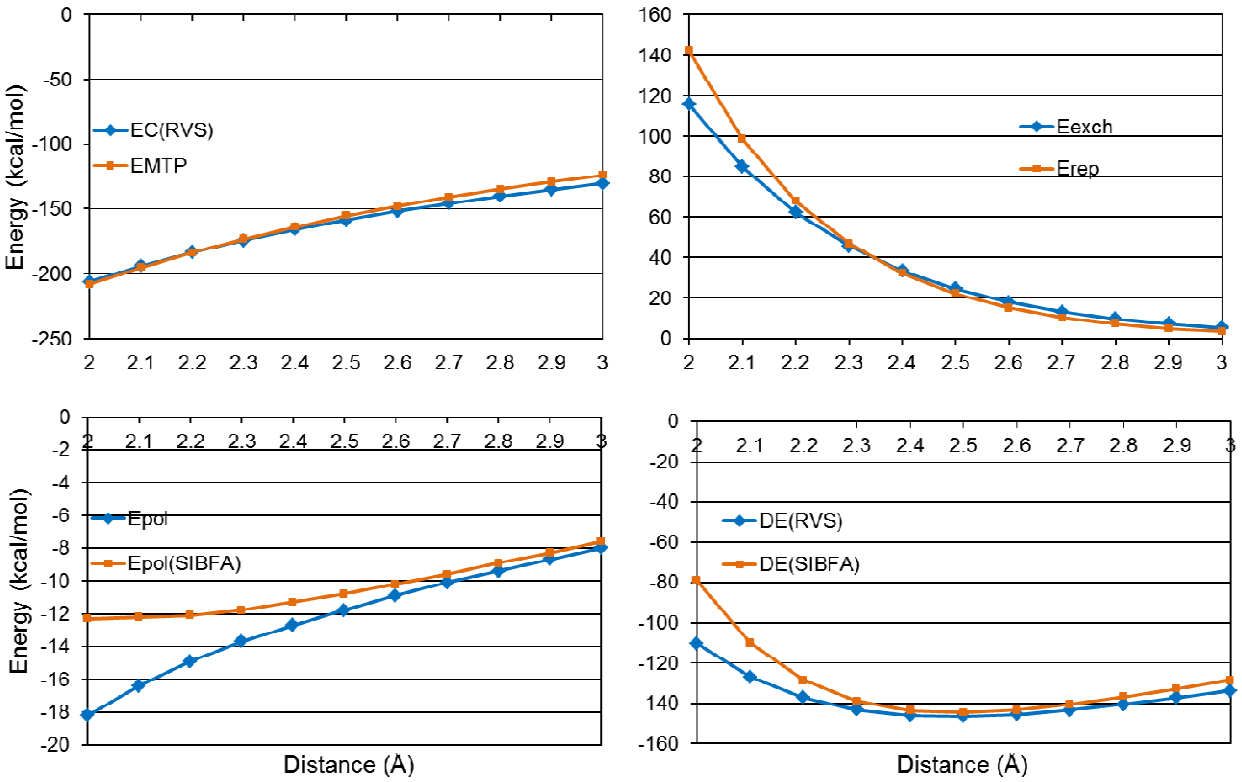

Figure 2a

er Review

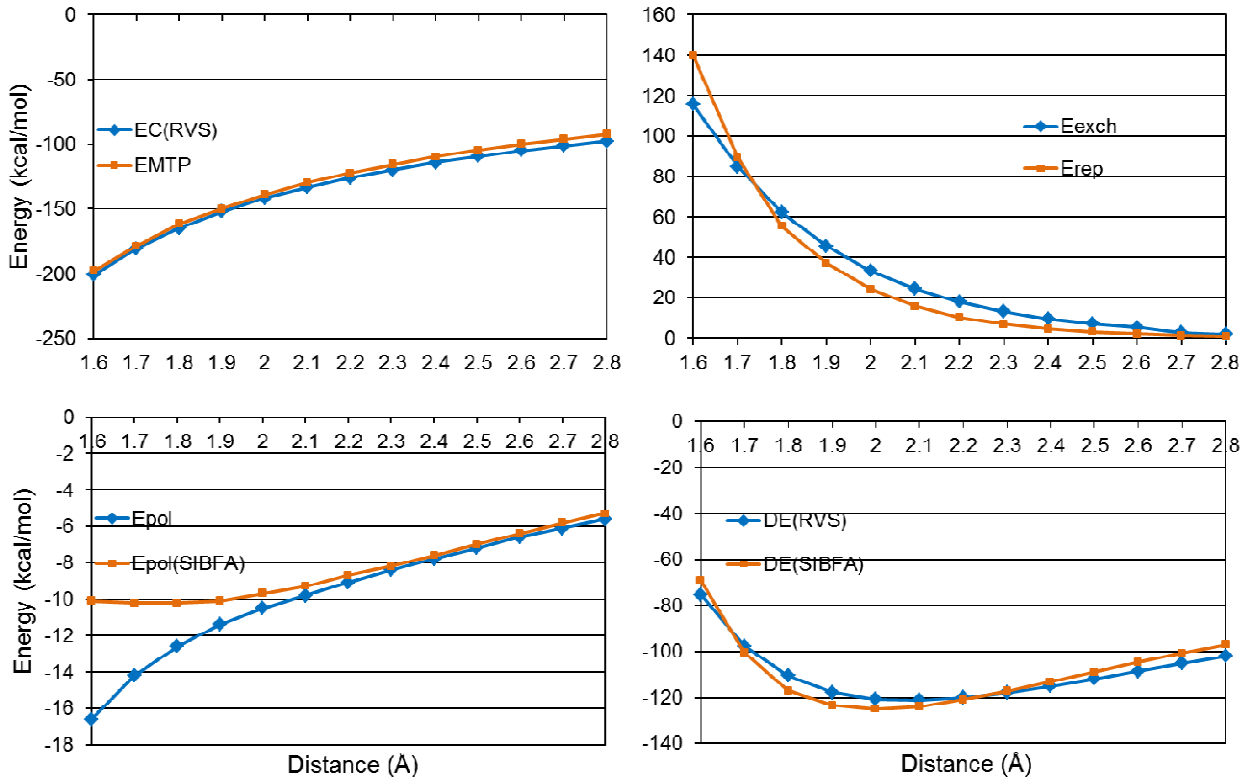

Figure 2b

er Review

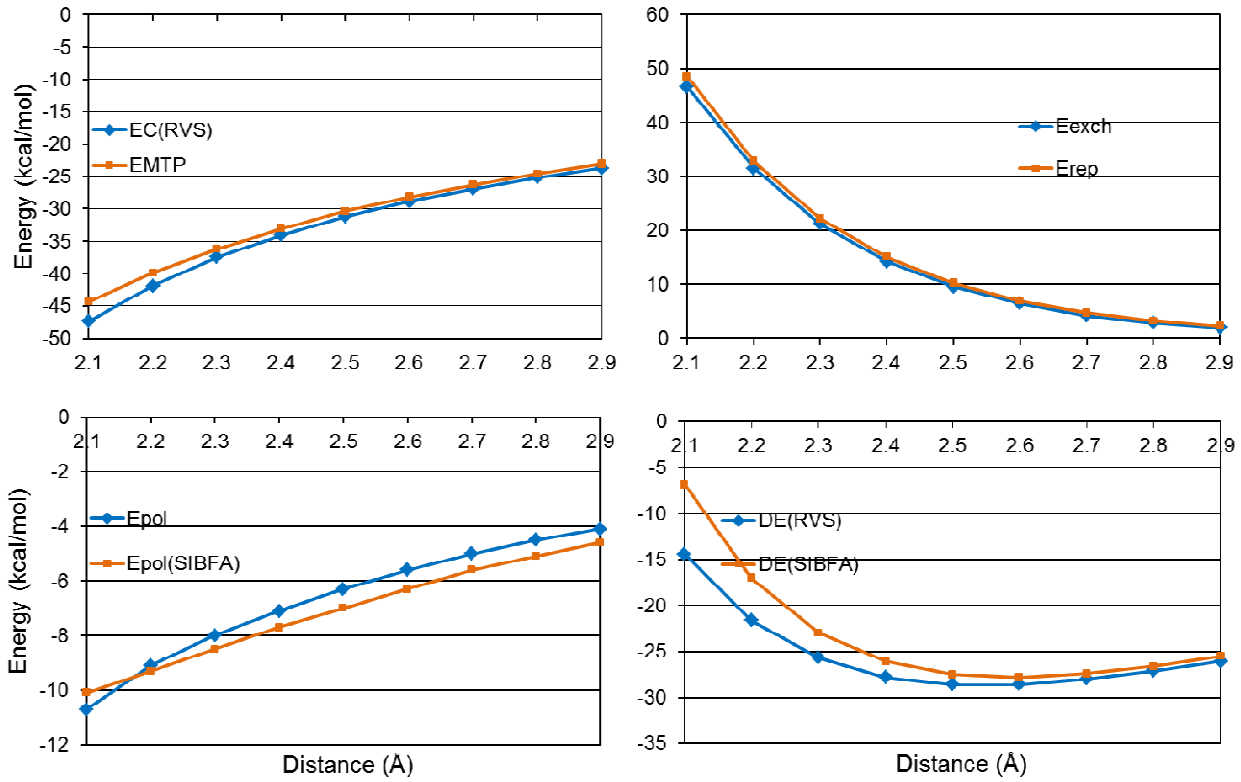

Figure 3

er Review

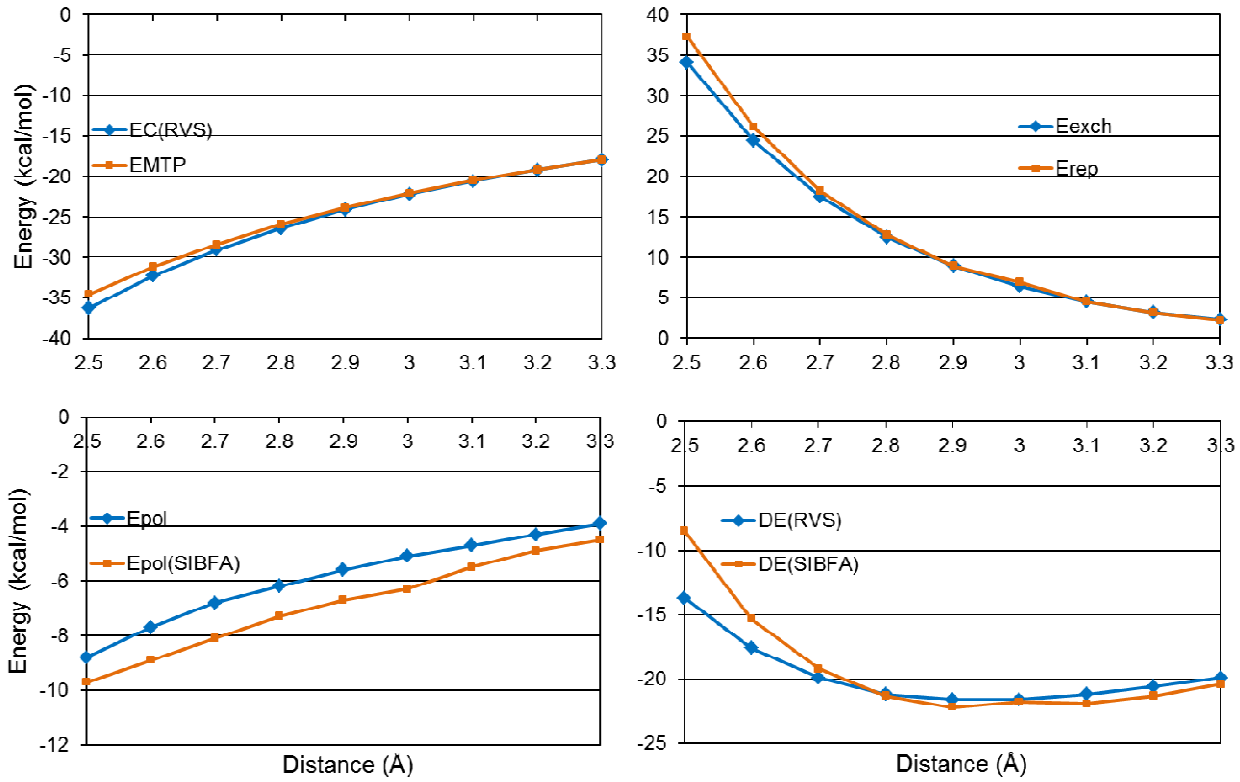

Figure 4

er Review

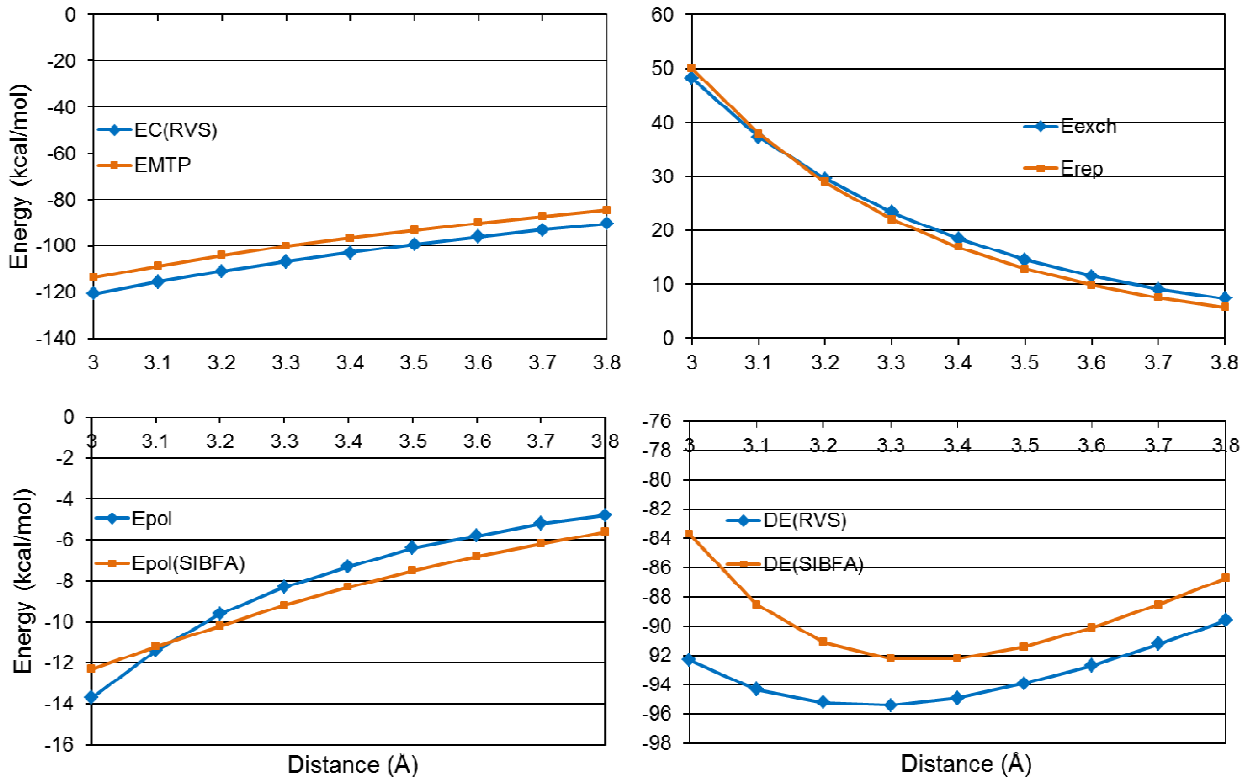

Figure 5

er Review

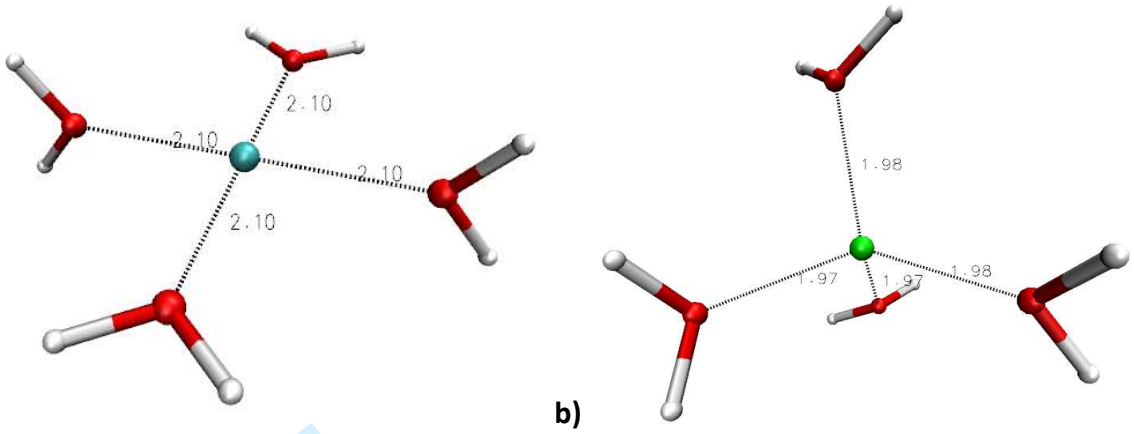

Figure 6

For Peer Review

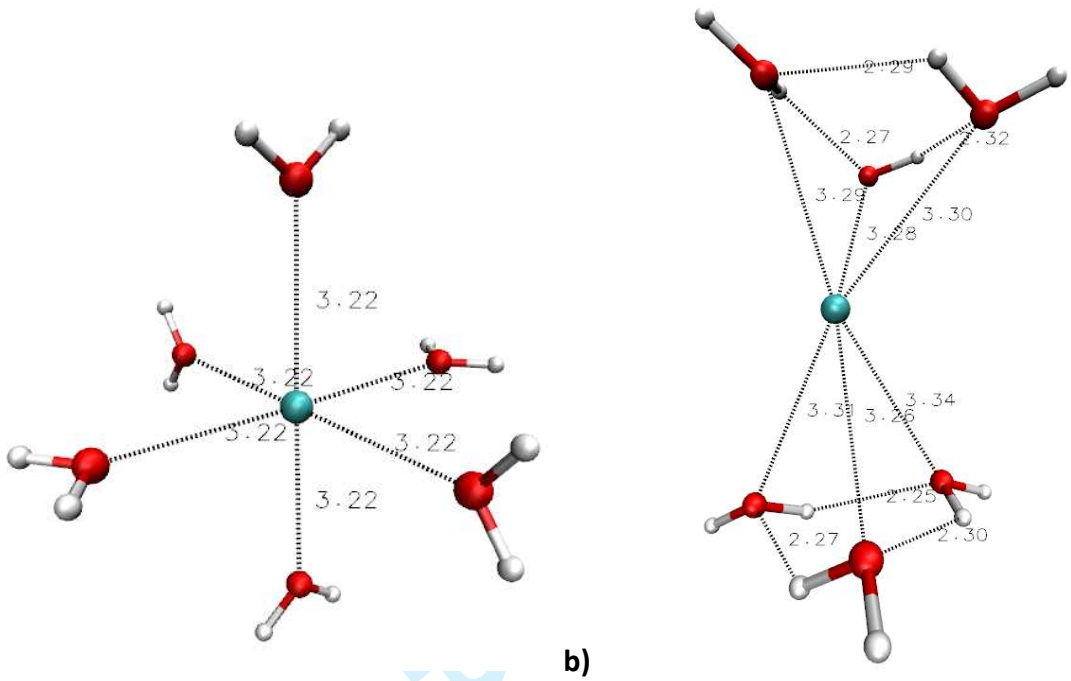

a) b)

Figure 7

Peer Review

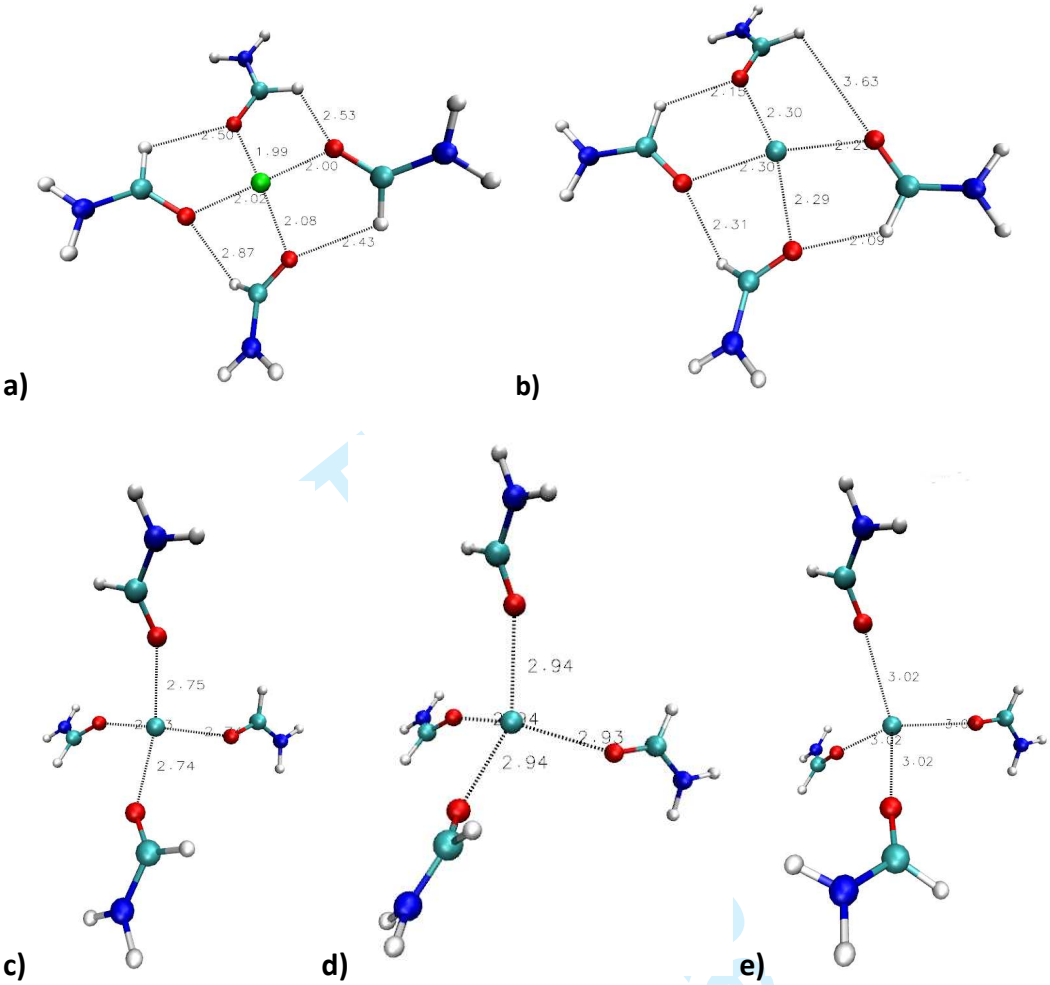
2.53
1.99
2.00
2.08
2.87
2.43
3.63
2.30
2.30
2.29
2.31
2.75
2.74
2.94
2.93
2.94
3.02
3.02
3.02
a)
b)
c)
d)
e)

Figure 8

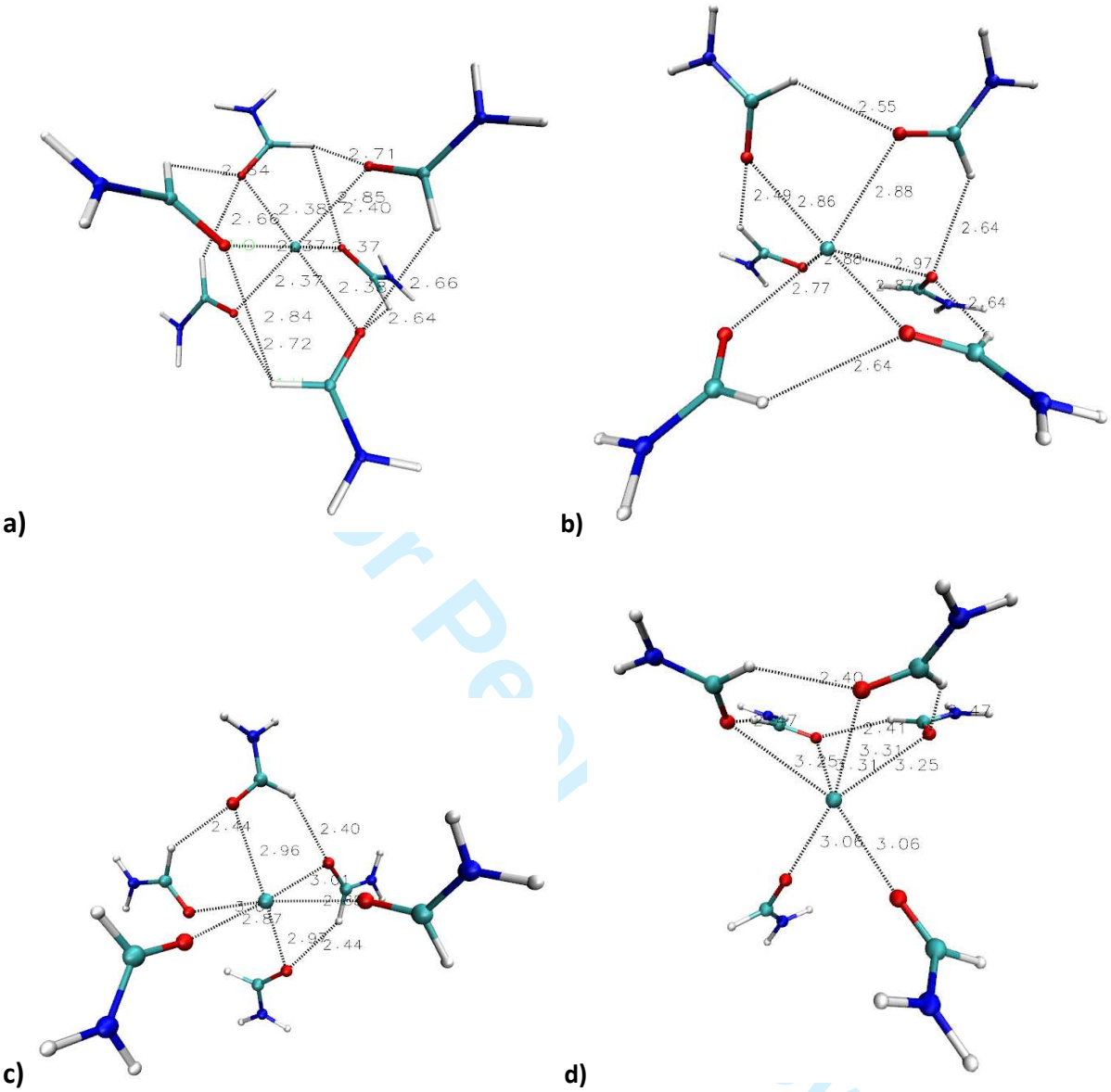

Figure 9

Supplementary Information

Supp. Info S1a. Monoligated Li+ complexes. Values (kcal/mol) of the correlated QC and SIBFA interaction energies and their contributions.

Oxygen ligands

	H2O, d=1.80		CH3OH, d=1.8		Formamide, d=1.70		Formate bridge, d=2.10		Formate external, d=1.70	
	QC	SIBFA	QC	SIBFA	QC	SIBFA	QC	SIBFA	QC	SIBFA
EC/EMTP*	-33.7	-34.7	-34.4	-33.7	-46.8	-47.6	-176.5	-168.8	-157	-148.1
Eexch/Erep	14	14.4	15.1	15.5	17.9	21.1	45.1	38.2	48.4	32
E1	-19.8	-20.3	-19.3	-18.3	-28.9	-26.5	-131.5	-130.6	-108.6	-116.1
Epol	-12	-12.9	-14.6	-16.7	-23.5	-17.8	-33.9	-39.4	-32.3	-22.9
Ect	-2.7	-1.8	-2.8	-1.9	0	-1.6	-5.2	-5.1	-6.1	-5
DE	**-34.6**	**-35**	**-36.9**	**-36.9**	**-52.7**	**-45.9**	**-169.9**	**-175**	**-147.5**	**-144**

Nitrogen and sulfur ligands

	imidazole, d=1.90		Methanethiolate, d=2.20 A	
	QC	SIBFA	QC	SIBFA
EC/EMTP*	-47.8	-41	-151.2	-156.3
Eexch/Erep	18.6	17.4	27	28.4
E1	-29.2	-23.6	-124.2	-128
Epol	-18.5	-20.3	-21.8	-33
Ect	-3.7	-2.9	-7.1	-3.4
DE	**-51.8**	**-46.9**	**-153.9**	**-164.3**

Supp. Info S1b. Monoligated Na+ complexes. Values (kcal/mol) of the correlated QC and SIBFA interaction energies and their contributions.

Oxygen Ligands

	H2O, d=2.20		CH3OH d=2.20		Formamide, d=2.10		Formate bridge, d=2.50		Formate external, d=2.00	
	QC	SIBFA	QC	SIBFA	QC	SIBFA	QC	SIBFA	QC	SIBFA
EC/EMTP*	-25.7	-26.4	-25.9	-25.9	-37.7	-37.2	-158.8	-156.7	-142.3	-138.5
Eexch/Erep	8.9	9.2	9.8	10.1	11.2	13.6	41.3	28.4	47.7	29.8
E1	-16.7	-17	-16.1	-15.8	-26.5	-23.6	-117.6	-128.3	-94.6	-108.7
Epol	-6.4	-6.6	-8.2	-8.8	-11.2	-14	-25.5	-20.5	-26.8	-12.9
Ect	-0.2	-0.1	-0.1	-0.1	0	-0.1	-0.7	-0.3	-0.7	-0.3
DE	**-23.5**	**-23.6**	**-24.6**	**-24.7**	**-37.9**	**-37.7**	**-144.9**	**-149.1**	**-122.8**	**-121.9**

Nitrogen and sulfur ligands

	imidazole, d=2.30		Methanethiolate, d=2.50 A	
	correlated QC	SIBFA	correlated QC	SIBFA
EC/EMTP*	-37.3	-33.6	-143.9	-138.8
Eexch/Erep	12.7	12.7	29.1	28
E1	-24.6	-20.8	-114.8	-110.7
Epol	-11.4	-11.1	-15.5	-19.4
Ect	-0.2	-0.1	-2	-0.2
DE	**-36.5**	**-32.1**	**-133.4**	**-130.4**

For Peer Review

Supp. Info S1c. Monoligated K+ complexes. Values (kcal/mol) of the correlated QC and SIBFA interaction energies and their contributions.

Oxygen ligands

	H2O, d=2.70		CH3OH d=2.70		Formamide, d=2.60		Formate bridge, d=2.90		Formate external, d=2.40	
	QC	SIBFA	QC	SIBFA	QC	SIBFA	QC	SIBFA	QC	SIBFA
EC/EMTP*	-17.2	-16.8	-16.9	-16.1	-26.7	-24.8	-137.9	-129.4	-117.4	-110.7
Eexch/Erep	4.6	5.1	5	5.7	6.4	7.1	41	26.1	40	22.5
E1	-12.6	-11.7	-11.9	-10.4	-20.3	-17.7	-96.9	-103.3	-77.3	-88.2
Epol	-3.2	-4.1	-4.4	-5.7	-6.3	-9.1	-21.3	-16.1	-23.4	-10.8
Ect	-0.2	-0.2	-0.2	-0.3	0	-0.2	-1.5	-1.5	-1.6	-1.4
DE	**-16.1**	**-16**	**-16.7**	**-16.3**	**-26.8**	**-27**	**-121.6**	**-120.9**	**-104.1**	**-100.4**

Nitrogen and sulfur ligands

	imidazole, d=2.80		Methanethiolate, d=2.90 A	
	correlated QC	SIBFA	correlated QC	SIBFA
EC/EMTP*	-24.9	-21.7	-121.6	-114.7
Eexch/Erep	6.9	7.4	25.4	23.8
E1	-18.1	-14.3	-96.2	-91
Epol	-6.5	-7.5	-21.8	-15.6
Ect	0.5	-0.3	-9	-1.5
DE	**-25.3**	**-22.1**	**-109.9**	**-107.9**

Supp. Info S1d. Monoligated Rb+ complexes. Values (kcal/mol) of the correlated QC and SIBFA interaction energies and their contributions.

Oxygen ligands

	H2O, d=3.00		CH3OH, d=2.90		Formamide, d=2.70		Formate bridge, d=3.10		Formate external, d=2.60	
	QC	SIBFA	QC	SIBFA	QC	SIBFA	QC	SIBFA	QC	SIBFA
EC/EMTP*	-13.8	-13.9	-14.7	-14.4	-25.7	-24.4	-129.3	-121.1	-108.6	-102.6
Eexch/Erep	2.8	3.2	4.9	5.5	7.4	8	37	25.8	35.4	21.6
E1	-11	-10.7	-9.7	-8.9	-18.3	-16.4	-92.3	-95.3	-73.2	-81.1
Epol	-2.4	-2.9	-3.7	-4.6	-5.9	-8.2	-20.4	-12.1	-22.7	-8.1
Ect	-0.2	-0.3	-0.1	-0.4	0	-0.5	-1	-1.8	-1.6	-1.8
DE	**-13.6**	**-13.8**	**-13.8**	**-13.9**	**-24.5**	**-25.1**	**-116.4**	**-109.2**	**-99.2**	**-98.9**

Nitrogen and sulfur ligands

	imidazole, d=3.00		Methanethiolate, d=3.10 A	
	correlated QC	SIBFA	correlated QC	SIBFA
EC/EMTP*	-21.9	-19.3	-113.4	-106.7
Eexch/Erep	6.2	6.3	23	21.1
E1	-15.7	-12.9	-90.4	-85.6
Epol	-5.5	-6.2	-7.6	-13.4
Ect	-0.5	-0.5	-4.1	-3.7
DE	**-21.9**	**-19.6**	**-103.6**	**-102.6**

For Peer Review

Supp. Info S1e. Monoligated Cs+ complexes. Values (kcal/mol) of the correlated QC and SIBFA interaction energies and their contributions.

Oxygen ligands

	H2O, d=3.10		CH3OH, d=3.10		Formamide, d=2.90		Formate bridge, d=3.20		Formate external, d=2.70	
	QC	SIBFA	QC	SIBFA	QC	SIBFA	QC	SIBFA	QC	SIBFA
EC/EMTP*	-13.4	-13.8	-13.1	-13.1	-23.3	-22.4	-127.4	-119.4	-106.6	-100.6
Eexch/Erep	4.2	4.3	4.5	5	6.8	7.1	43.7	34.4	41.3	27.6
E1	-9.3	-9.5	-8.5	-8.1	-16.5	-15.3	-83.8	-85.1	-65.2	-73.9
Epol	-2.2	-2.6	-3.1	-3.7	-5.3	-6.6	-21.1	-10.9	-23.8	-7.3
Ect	-0.2	-0.4	-0.2	-0.4	0	-0.5	-2.1	-2.6	-1.8	-2.4
DE	**-11.8**	**-12.4**	**-12**	**-12.2**	**-22**	**-22.4**	**-110.5**	**-98.6**	**-93.9**	**-82.7**

Nitrogen and sulfur ligands

	imidazole, d=3.10		Methanethiolate, d=3.30 A	
	correlated QC	SIBFA	correlated QC	SIBFA
EC/EMTP*	-21.1	-18.8	-105.5	-100
Eexch/Erep	8.5	8	22.5	22.5
E1	-12.6	-26	-83	-77.6
Epol	-5.5	-5.6	-8.2	-11.2
Ect	-0.6	-0.7	Unconverged	-4.6
DE	**-19.2**	**-17.1**		**-93.4**

For Peer Review